Effects of elephant densities on landscape heterogeneity in relation to surface water availability: A GIS and remote sensing-based approach

By

Zorodzai Dzinotizei (R081021E)

Thesis submitted to the Department of Geography and Environmental Science, University of Zimbabwe, in fulfilment of the requirements for the Master of Philosophy degree in Geography and Environmental Science (Spatial Ecology)

September 2018

Abstract

Predictions have been made on the effect of increased elephant *(Loxodonta africana)* densities on landscape heterogeneity change as a result of artificial waterholes in semi-arid savanna landscapes of southern Africa. However, limited effort has been put forth to test these predictions spatially. This thesis sought to test the utility of a Geographic Information System (GIS) and remote sensing-based approach to understand the effects of elephant density on landscape heterogeneity change around artificial waterholes in Hwange National Park (HNP). Firstly, an objective method based on satellite remotely-sensed data was tested for efficiency in detecting and mapping waterholes at an optimal threshold. In this regard, the performance of the Modified Normalised Difference Water Index (MNDWI) and newly developed Superfine Water Index (SWI) were evaluated at selected optimal thresholds, using Landsat image data. Kappa coefficient results indicated that the MNDWI detects waterholes better than the SWI and that the optimal threshold for detecting waterholes using MNDWI is -0.29. The study further validated accuracy of MNDWI-detected waterholes using spatial and temporal rainfall data and tested for aridity, using the remotely-sensed waterholes. Secondly, the study related the spatial distribution of waterholes detected using MNDWI to elephant density and assessed short-term (seasonal scale) elephant density effects on vegetation heterogeneity change using the coefficient of variation of the Normalised Difference Vegetation Index (NDVI CoV). It also assessed long-term elephant density effects as a result of artificial waterholes on landscape heterogeneity change using landscape metrics. The study also tested the potential influence of an existing spatial rainfall gradient on landscape heterogeneity change. Results show that density of elephants is significantly influenced by spatial distribution of waterholes in the late dry season. Results show that in the short-term there is no relationship between NDVI CoV change and elephant density. In the long term, results show that woodland mean patch size, woodland class proportion and bushland patch density decrease while bushland mean patch size and bushland class proportion increase with increasing density of artificial waterholes. Results suggest that consistently high elephant density in the area with high artificial waterhole density leads to a decrease in woody vegetation structural diversity as woodland patches are converted to bushland as a result of coppicing due to intensive browsing by elephants. However, homogenisation of vegetation in the landscape is being inhibited by other mediating factors which are converting bushland to grassland. Results provide evidence that landscape heterogeneity dynamics in HNP are not significantly influenced by spatial rainfall variability. In conclusion, this thesis demonstrated that GIS techniques and remotely-sensed data can effectively be used to detect and map waterholes, assess waterhole-elephant density dynamics and quantify elephant density effects on landscape heterogeneity change over short and broad temporal intervals for sustainable management of semi-arid savanna ecosystems.

Dedication

To my family, your encouragement and continual support is beyond comparison. We share this accomplishment together!!!

I thank the Lord for His guiding hand that has led me in so many ways…

Declaration 1: Originality

I do hereby declare that this thesis submitted for the Master of Philosophy degree at the University of Zimbabwe is my original work and has not been previously submitted to any other institution of higher education. I further declare that all sources cited and quoted are shown by means of a comprehensive list of references.

Dzinotizei Zorodzai

Declaration 2: Publications

Details that form part and/or presented in this thesis include published articles and/or submitted manuscripts:

Publication 1: Zorodzai Dzinotizei*[1], Amon Murwira[1], Fadzai M. Zengeya [1], Laure Guerrini[2] (2017). *Mapping waterholes and testing for aridity using a remote sensing water index in a southern African semi-arid wildlife area.* **Geocarto International,** 1-13. http://dx.doi.org/10.1080/10106049.2017.1343394

This work was conducted by the first author under the guidance and supervision of the other authors.

[1]Department of Geography and Environmental Sciences, University of Zimbabwe, P. O. Box MP 167, Mount Pleasant, Harare
[2]CIRAD, P. O. Box 1378, Harare, Zimbabwe

Publication 2: Zorodzai Dzinotizei*[1], Amon Murwira[1] and Mhosisi Masocha[1]
Elephant-induced landscape heterogeneity change around artificial waterholes in a protected savanna woodland ecosystem (Submitted to **Remote Sensing Applications: Society and Environment**)

This work was done by the first author, under the guidance and supervision of the second and third authors

[1]Department of Geography and Environmental Sciences, University of Zimbabwe, P. O. Box MP 167, Mount Pleasant, Harare, Zimbabwe

Certification by Supervisor (Prof Amon Murwira)

…….

Acknowledgements

I relay my sincere gratitude to the research and funding bodies that facilitated the successful completion of this study. This work was conducted within the framework of the Research Platform Production and Conservation in Partnership (RP-PCP). I heartily thank the French Agence Nationale pour la Recherche for supporting this research work through the SAVARID project (ANR-11-CEPL-003 SAVARID). I am grateful for the financial grant from the German Academic Exchange Service (DAAD) awarded towards this research project. Special thanks also go to the University of Zimbabwe for offering me the opportunity to carry out my MPhil study and also assisting me with funding for this research.

I deeply thank my supervisors Professor Amon Murwira and Professor Masocha. I will always be indebted to Professor Murwira, for the steadfast support throughout this challenging journey. Thank you for the positive words of affirmation and the goal-getting attitude that essentially revitalised me during low spells in my studies. The research skills and knowledge you imparted to me are priceless. Thank you for your dedication. My earnest gratitude goes to Professor Masocha for the constructive ideas you gave me during the course of my studies to help improve the quality of this work. I sincerely thank Dr Zengeya for the scrupulous review and refinement of ideas in this study. I am grateful to Dr Guerrini for the helpful scholarly ideas and regular enquiries she made on my progress. I also thank Mr Ndaimani for the helpful scholarly corrections and Mr Mambambo for proofreading and editing this work. I am deeply indebted to the University of Zimbabwe's Department of

Geography and Environmental Science academic and technical staff; I gratefully acknowledge your varied yet immensely valuable contributions to my studies.

I reserve special thanks for my colleagues *Ratidzo Mapfumo, Charon Chikuruwo, Leoba Chigwenhese, Clarice Mudzengi, Farai Kuri, Farai Matawa, Trymore Muderere* and *Stanlake Mtetwa;* thank you for the shared hopes and motivation that were of great help to me along the way. Also to a precious and cherished category of friends, I thank you for your steadfast encouragement and support. Last but not least, I am mostly grateful to my parents and family; *baba* for the resolute support and concern shown in my studies, *mama* for the motherly care and encouragement you offered and to all the family members for the sacrifices made and all good wishes you blessed me with. May God bless you all.

List of acronyms

AWEI	Automated Water Extraction Index
EWI	Enhanced Water Index
GIS	Geographic Information System
GPS	Global Positioning System
HNP	Hwange National Park
MNDWI	Modified Normalised Difference Water Index
NDVI	Normalised Difference Vegetation Index
NDWI	Normalised Difference Water Index
SWI	Superfine Water Index
TAMSAT	Tropical Applications of Meteorological Satellites
TOA	Top of Atmosphere
WWF	World Wide Fund
ZPWMA	Zimbabwe Parks and Wildlife Management Authority

Table of contents Page

List of figures Page

List of tables Page

Chapter 1: General introduction

1.1 Background

Over the years, protected areas in southern Africa have seen a major increase in elephant *(Loxodonta africana)* population densities (Balfour et al., 2007) and this has been attributed to the provision of supplementary water from artificial waterholes (Chamaillè-Jammes et al., 2007c; Guldemond et al., 2017). To counter shortages in natural surface water availability for wildlife and to moderate extreme shortages of water during drought years, human intervention has facilitated provision of borehole-pumped water in pans i.e. artificial waterholes in semi-arid protected areas of southern Africa (Owen-Smith, 1996; Gaylard et al., 2003; Davidson et al., 2013). During the dry season when most natural water sources dry up, elephants have been observed to stay close to the artificial water sources to adequately meet their drinking needs (Chamaillè-Jammes et al., 2009b; Shrader et al., 2010). However, dependence on artificial waterholes has induced changes in distribution patterns of elephants, with the elephants aggregating around artificial waterholes and increasing local elephant densities in these areas (Chamaillé-Jammes et al., 2007c; Kalwij et al., 2010).

Specifically, it is largely hypothesised that elephant densities exceed the ecological carrying capacity of certain areas where there is high artificial waterhole density (Cumming et al., 1997; Van Aarde and Jackson, 2007). This has given rise to many hypotheses, the main one

being that increased elephant densities will result in over browsing (Western and Maitumo, 2004). The destructive feeding patterns of elephants on woody vegetation (debarking, uprooting trees and branch breaking), coupled with high elephant densities may result in whole landscapes being transformed (Whyte et al., 2003; Shrader et al., 2010). At high densities elephants are capable of reducing tree density, transforming trees to short dense shrubs and decreasing overall woody vegetation structural diversity (Whyte et al., 2003; Fullman and Bunting, 2014; Guldemond et al., 2017), resulting in a changed landscape structure (Baldi and Paruelo, 2008; Shannon et al., 2009) and consequently habitats of other wildlife species. Semi-arid protected areas serve as sanctuaries for a range of endangered and threatened wildlife species. These protected species require sufficient conservation through the effective supply of water and maintenance of suitable habitat. Thus, the need to test how different elephant densities impact landscape heterogeneity change is critical to conservation of biodiversity.

Although the hypothesis that elephant densities have increased around artificial waterholes thereby affecting landscape heterogeneity has been proposed, limited effort has been made to test these predictions spatially at the landscape scale in semi-arid savanna ecosystems of southern Africa. Consequences of high elephant density on changes in spatial patterns of vegetation are complex (Murthy et al., 2003; Fullman and Child, 2012). For instance, Owen-Smith (2006) observed that while some areas were intensively degraded, the vast part of the protected areas seemed ecologically intact, thus providing evidence for this complexity. Testing this hypothesis using spatial methods will allow comprehensive ecological deductions to be made on the effect of elephant densities on landscape heterogeneity change.

1.2 Problem statement and Hypothesis

Assessing the effect of elephant density on surrounding landscape heterogeneity change and the influence of spatial distribution of artificial waterholes on elephant movement and distribution at the landscape scale relies upon successful detection of waterholes. To date, work which has so far tested for a remote sensing-based method and the optimal threshold best suited to detecting waterholes is still rudimentary. A number of spectral water indices for detecting larger surface water features (lakes, dams, freshwater reservoirs) have been developed: Automated Water Extraction Index (AWEI) (Feyisa et al., 2014); Normalised Difference Water Index (NDWI) (McFeeters, 1996); Modified Normalised Difference Water Index (MNDWI) (Xu, 2006) and Enhanced Water Index (EWI) (Ayana et al., 2015). However, the optimal threshold for detecting small water features such as waterholes using a more robust spectral water index still remains under-tested. Successful detection of waterholes using a remote sensing-based water index depends on assessing robustness of existing spectral water indices and even new ones developed and on the selection of optimal thresholds for detecting surface water (Xu, 2006; Li et al., 2013). In this regard, this thesis tested for a robust remotely-sensed water index at an optimal threshold for effectively detecting and mapping waterholes.

Several studies in protected areas have quantified the impacts of elephants on vegetation in relation to surface water. However, these have been limited to assessment of elephant distribution and associated woody cover change in relation to water proximity and distribution (Thrash and Derry, 1999; Brits et al., 2002; Kalwij et al., 2010; Fullman and Child, 2012; Landman et al., 2012; Mukwashi et al., 2012). These studies have mainly been

done using cost and time intensive fieldwork and were also conducted on smaller spatial and temporal scales which do not adequately capture spatial dynamics of the landscape in the long term.

This study hypothesises that that increasing elephant densities as a result of artificial waterholes amplifies elephant impacts on vegetation leading to changes in landscape heterogeneity. To test this hypothesis, this study made use of freely available satellite remotely sensed data and Geographic Information System (GIS) techniques, combined with elephant density data from aerial surveys, to quantify elephant density effects on vegetation heterogeneity change around artificial waterholes at the landscape scale. The proper quantification of the effects of elephant densities as a result of artificial waterholes on landscape heterogeneity change based on GIS and remote sensing methods is critical for management of semi-arid protected areas.

1.3 Thesis objectives

The main objective of this thesis was to test the utility of GIS and remote sensing-based approaches to understand the effects of elephant density on landscape heterogeneity change around artificial waterholes.

Specific objectives were:

- To develop an objective method for detecting and mapping waterholes using satellite remotely-sensed data
- To assess the relationship between remotely-sensed waterholes and elephant densities

- To assess the short-term and long-term elephant density effects on vegetation cover and landscape heterogeneity change around artificial waterholes

1.4 Significance of research

The purpose of this study was to evaluate vegetation change as a result of artificial waterhole provision using GIS and remote sensing methods. This will guide policy formulation and management decisions for supplementing natural water sources with artificial waterholes while taking into consideration the impact this will have on elephant distribution patterns and landscape heterogeneity change for conservation of wildlife and their habitats.

1.5 Organisation of the thesis

This thesis is divided into four chapters which include two papers. This structure allows chapters to be read separately. However, there is repetition of some information between chapters, but this is considered of minimum distraction in the flow of the thesis since the structure enhances clarity when each chapter is read independently.

Chapter 1 describes the background of the study i.e. the establishment of artificial waterholes in semi-arid protected areas; concerns over increased elephant densities and elephant-induced landscape heterogeneity change. The chapter highlights the purpose of the study to map waterholes and quantify elephant density effects on landscape heterogeneity change using satellite remote sensing and GIS methods. The chapter further outlines specific objectives of the thesis.

Chapter 2 tests for robustness of two remote sensing water indices in detecting and mapping waterholes at optimum thresholds and as a way of validating the remotely-sensed waterholes, assessing spatial and temporal dynamics of these in relation to spatial and temporal rainfall patterns and then testing for aridity using remotely-sensed waterholes.

Chapter 3 tests for the relationship between spatial distribution of waterholes mapped using a robust remote sensing water index and elephant densities and the effect of different elephant densities on landscape heterogeneity change in the short-term and long-term using the coefficient of variation of the Normalised Difference Vegetation Index and landscape metrics, respectively. The influence of spatial rainfall variability on landscape heterogeneity change is also evaluated.

Chapter 4 is a synthesis of the major findings of the thesis. Specifically, this chapter discusses the scientific output generated in the thesis in mapping waterholes and quantifying effects of elephant density on landscape heterogeneity change using remotely-sensed data and GIS methods and the management implications of the findings of this thesis. The candidate concludes the chapter by discussing the limitations of the research and recommendations for future research.

Chapter 2: Mapping waterholes and testing for aridity using a remote sensing water index in a southern African semi-arid wildlife area

---

This chapter is based on: **Zorodzai Dzinotizei, Amon Murwira, Fadzai M. Zengeya, Laure Guerrini (2017).** *Mapping waterholes and testing for aridity using a remote sensing water index in a southern African semi-arid wildlife area.* **Geocarto International,** *1-13.*

Abstract

Waterholes are a key resource that influences wildlife distribution in semi-arid ecosystems. Mapping waterholes can guide intervening decisions for supplementing water resources and managing wildlife distribution patterns. Although remote sensing provides a key to mapping distribution of waterholes, efficiency of existing remotely-sensed methods for detecting waterholes have to be evaluated and even new ones developed. This study evaluated performance of MNDWI and SWI at selected optimum thresholds. Performance of the two water indices in detecting waterholes was evaluated using the Kappa coefficient which measures the agreement between the binary classified image and test data (observed values) while correcting for chance agreements. Kappa results indicated that MNDWI detects waterholes better than SWI. MNDWI-detected waterholes were further validated by testing response of waterhole area to annual temporal rainfall and waterhole persistence to spatial rainfall where surface water is expected to be related to rainfall in semi-arid areas. Extent of MNDWI-detected waterholes varied in relation to temporal rainfall variability ($P < 0.05$). Waterhole persistence was not associated with spatial rainfall variability which could be explained by differences in waterhole types, low spatial rainfall variability or a range of factors such as differences in percolation, size of pans or animal activity

2.1 Introduction

In semi-arid areas, waterholes are a life-sustaining water source for most wildlife species. Waterholes are a key driver of the dry savanna ecosystem and in natural settings, their presence is often determined by annual rainfall (Chamaillé-Jammes et al., 2007a; Shrader et al., 2010). The spatial distribution of waterholes often drives wildlife population dynamics (Young et al., 2009; Simpson et al., 2011; Fullman and Child, 2012). In fact, in dry years, massive die-offs of wildlife species have been known to occur, due to severe shortages of drinking water and grazing (Dudley et al., 2001). To this end, understanding trends and distribution patterns of waterholes is important to the management of wildlife.

Remote sensing is regarded as one of the most appropriate approaches to detect and map waterholes in different environments. Remote sensing allows observation and systematic monitoring of waterholes at regular temporal intervals and large spatial extents which would otherwise be cost and time intensive using traditional field-based methods of surveying and mapping waterholes (Senay et al., 2013). However, the success of remote sensing in the detection of waterholes requires the development and/or adoption of appropriate methods (Deus and Gloaguen, 2013). To date, several remotely sensed indices have been used to detect surface water in the landscape: NDWI (McFeeters, 1996); MNDWI (Xu, 2006); AWEI (Feyisa et al., 2014); and EWI (Ayana et al., 2015). Among these remotely sensed indices, the MNDWI has proved to be more superior in delineating water (Hui et al., 2008; Ji et al., 2009; Deus and Gloaguen, 2013; Li et al., 2013; Singh et al., 2015). However, the SWI has also been touted as highly sensitive to surface water, at the global scale compared to former water detecting indices (Sharma et al., 2015). Yet the successful detection of waterholes using a water index depends on the selection of appropriate thresholds (Xu, 2006). While

several surface water detecting thresholds have been proposed (Ji et al., 2009), to the best of the candidate's knowledge no particular optimal threshold has been tested and proposed for detecting active waterholes in semi-arid regions such as those of southern Africa.

Temporal trends in waterhole extent and spatial dynamics in waterhole persistence in the landscape are often a result of dynamics in rainfall especially in semi-arid regions (Gaylard et al., 2003). One of the ways of further validating remotely-sensed waterhole existence is to use rainfall data to test whether the waterhole dynamics are related to rainfall using multi-temporal data. Since waterhole dynamics are related with rainfall in semi-arid regions, it is reasonable to expect that there is a significant association between dynamics in remotely-sensed waterholes and rainfall. To the best of the candidate's knowledge, a few or no studies have used multi-temporal and spatial rainfall data to validate accuracy of remotely-sensed waterholes.

This study tested the capability of Landsat satellite imagery-based SWI and MNDWI to detect waterholes in HNP, northwest Zimbabwe. Specifically, the study tested for the existence of a SWI and MNDWI threshold that could be used to improve the detection of waterholes. Temporal trends in waterhole extent were tested, in the light of predictions of a reduction in annual rainfall and increase in drought frequency in semi-arid regions of Africa (Shrader et al., 2010). Next, to validate accuracy of remotely-sensed waterholes detected using the better performing water index, the study tested whether there is evidence of significant variability in waterhole extent in relation to temporal rainfall variation and also variability of waterhole persistence, in relation to spatial rainfall variation in HNP.

2.2 Materials and methods

2.2.1 Study site

The study area was Hwange National Park, in northwest Zimbabwe, which is roughly situated between latitudes 18° S and 20° S and longitudes 25° 4' E and 27° 4' E. It covers an area of 14 651km^2 (Figure 2.1). This region belongs to the semi-arid, bioclimatic domain of Zimbabwe where rainfall ranges between 300 and 800mm annually and the average yearly temperature is between 20 and 30°C. The climate is characterised by a short wet season from November to March and a long dry season from April to November. Rainfall varies seasonally and is patchily distributed in space and time (Dudley et al., 2001).

In Hwange, densities of large herbivore (including elephants (*Loxodonta africana*), buffalo (*Syncerus caffer*), zebra (*Equus quagga*), giraffe (*Giraffa camelopardalis*), kudu (*Tragelaphus strepsiceros*), wildebeest (*Connochaetes taurinus)* and impala (*Aepyceros melampus*)) are important biodiversity components. Water is one of the main factors limiting resource availability and influencing wildlife abundance. The primary natural water sources for wildlife are waterholes and rivers. A greater proportion of these water sources dry up as the dry season progresses. Critical shortages of drinking water for wildlife are usually experienced in the dry season. To buffer shortages of natural surface water availability, the park authorities normally pump water from boreholes.

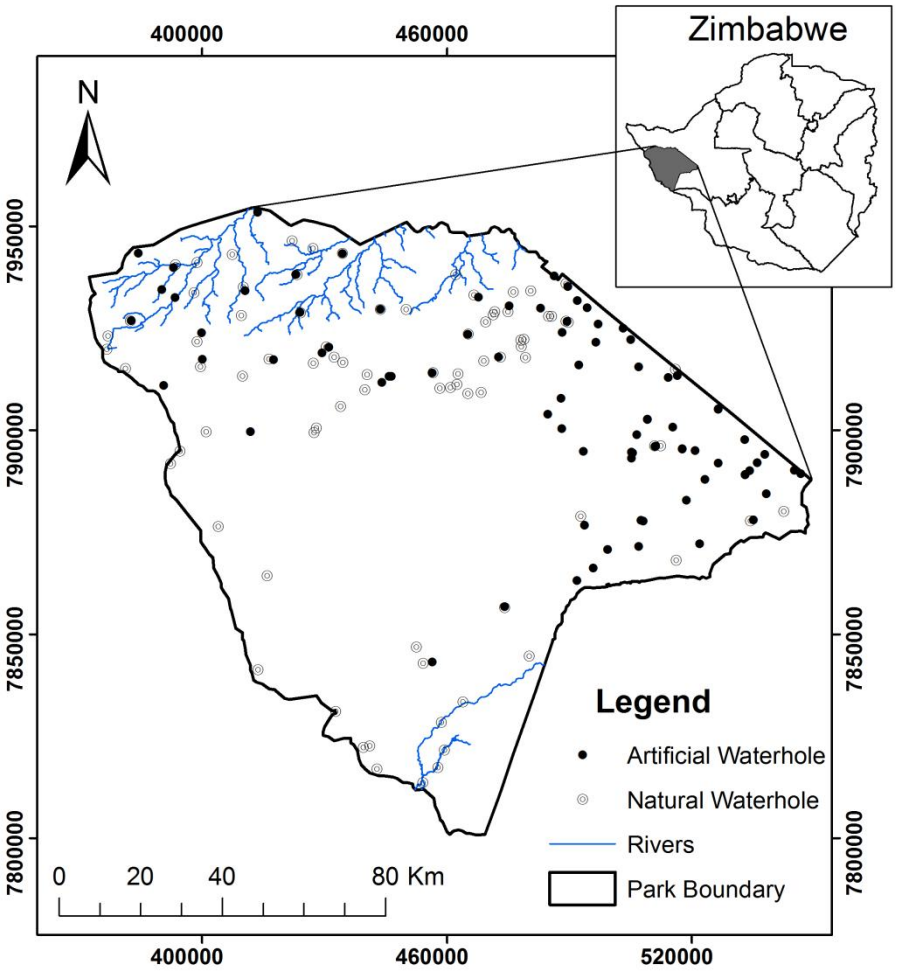

Figure 2.1 Map of Hwange National Park showing main surface water features. Map coordinates are in metres based on UTM zone 35 south, WGS 1984 spheroid

2.2.2 Remotely-sensed data and methods

2.2.2.1 Image acquisition and processing

Landsat images (5 Thematic Mapper (TM), 7 Enhanced Thematic Mapper plus (ETM +) and 8 Operational Land Imager (OLI)) with a spatial resolution of 30m were freely downloaded from www.usgs.gov website for the dry season period of 1990 to 2016. The dry season was considered to be from April–October and images were downloaded for this period except for the years 2000, 2003, 2005, 2008, 2010, 2011 and 2012 due to unavailability of data. Three

Landsat scenes (Path/Row 172/73, 172/74 and 173/73) were required to cover the study area. Prior to calculating indices for extracting water surfaces, radiometric correction was first performed, which involves converting the digital number of pixels to top of atmosphere reflectance (TOA) using ENVI 5.1 (ITT, 2013). This correction is deemed important especially when multi temporal analysis is performed. It allows comparison of images at different dates where sensor geometry, sun angle and atmospheric conditions will be inconsistent for separate images (Coppin et al., 2004; Schneier-Madanes and Courel, 2010). Next, the images were mosaicked and a subset of the images was created in a GIS by overlaying a mosaic with a mask created by digitising all areas considered as open depressions where water could collect and at some point in time function as waterholes and filled up depressions already identifiable as waterholes in HNP. Waterhole areas were digitised from accessible high resolution Landsat imagery made available through Google Earth (www.googleearth.com) within the period of study (1990–2016). All landcover surfaces outside of digitised waterhole areas were excluded from classification as there is often confusion in detection of cloud shadows, terrain shadows and highly vegetated swampy areas as surface water (Bochow et al., 2012; Du et al., 2012; Verpoorter et al., 2012; Nigro et al., 2014).

Waterhole areas considered were those at least 2025m^2 (45*45m) or more in area based on exploratory data analysis. The 45*45m dimension was deemed a suitable minimum size for detecting waterholes that can be reliably linked to scale, with the pixels of Landsat images which are 30*30m in area, while accommodating for the displacement in position of a waterhole to the fixed position of an image pixel (Lindquist and D'Annunzio, 2016). Artificial waterholes were also masked based on the Global Positioning System (GPS) location of artificial waterholes in HNP and excluded from analysis.

2.2.2.2 Waterhole detection

To identify the waterholes, two indices, the SWI proposed by Sharma et al., (2015) and the MNDWI proposed by Xu, (2006) were used. The SWI index was calculated as follows:

$$SWI = \frac{Sat_{(\mathrm{RGB})} - 7 \times NIR}{Sat_{(\mathrm{RGB})} + 7 \times NIR} \qquad \textbf{Equation 1}$$

where the 'Saturation (Sat)' is obtained from the (Hue–Saturation–Value) transformation of the RGB composite made up of red (R), green (G) and blue (B) bands of Landsat data. The 7.0 coefficient on the near infrared reflectance (NIR) was introduced in such a way that the raised near infrared reflectance does not reach the saturation values of the water areas (Sharma et al., 2015). The SWI can efficiently detect very narrow bodies of water, as well as extract water surfaces despite a variety of background objects and turbidity of water (Sharma et al., 2015).

The MNDWI is calculated as follows:

$$MNDWI = \frac{Green - MIR}{Green + MIR} \qquad \textbf{Equation 2}$$

where Green is a band such as TM band 2, ETM+ band 2, OLI band 3 and MIR is a middle infrared band such as TM band 5, ETM+ band 5 or MIR can be substituted by a shortwave infrared (SWIR) band such as OLI band 6. In fact, the spectral response of water is highly sensitive in the middle infrared band than in the near infrared band and this allows better detection of waterholes. Both spectral indices (SWI and MNDWI) typically give positive values for pixels representing water. Therefore the performance of SWI and MNDWI was

evaluated in detecting water features i.e. waterholes using Landsat data at selected optimal thresholds.

Preliminary field surveys were done in HNP but on a relatively small scale (25 waterholes were surveyed on the ground). Due to the large scale at which this study was done, waterhole data were acquired from high resolution images made available through Google Earth. For waterhole presence modelling and validating, data on water presence and absence was collected from high resolution Landsat images made available through Google Earth (www.googleearth.com) for April–May 2016. For the previous years (pre-2016) some of the high resolution image dates coincided with dates when Landsat data were not available while some historical scenes were not fine enough to accurately distinguish water presence from absence. In order to evaluate the performance of the two indices in extracting water surfaces, the dry season MNDWI and SWI images for 2016 were considered as this period coincided with dates when data were captured using high resolution Landsat images.

Using 460 randomly selected training points (which represented 70% of water presence and absence data collected from high resolution images), values of MNDWI and SWI were extracted at location of waterholes where water was either present or absent. The Binary Logistic regression model was used to compute the relative significance of MNDWI and SWI to predict the probability of water presence. An equal number of surface water presence and absence points was used for model building, to minimise bias towards the larger group of sampled points (Liu et al., 2005).

2.2.2.3 Optimal threshold

Optimal thresholds were determined from waterhole presence modelling using probability of waterhole presence. For binary classification of the image to a presence and absence map, the threshold was continuously adjusted based on visual valuation. From the adjustments, the most applicable cut-off point was the value which minimised the Euclidean distance between probability curve and the upper left corner of the probability graph, similar to the position of an optimal threshold from a ROC curve (Cantor et al., 1999). The cut-off value also corresponded to 95% probability of waterhole presence.

In addition, 30% of withheld points on surface water presence and absence acquired from high resolution images made available through Google Earth were used as test data for validating performance of MNDWI and SWI models in detecting surface water. The SWI and MNDWI images for 2016 were classified using the optimal thresholds computed for SWI and MNDWI. The test points were overlaid on the classified MNDWI and SWI images and a confusion matrix to describe performance of each classification model was generated. The Kappa coefficient which measures the agreement between the classified image (predicted values) and test data (observed values) while correcting for chance agreements (Jenness and Wynne, 2005) was calculated to evaluate the performance of the SWI and MNDWI in detecting surface water at optimal thresholds. The Kappa statistic was calculated as:

$$Kappa = \frac{P_o - P_e}{1 - P_e} \qquad \textbf{Equation 3}$$

Where P_o is the observed proportion of agreement and P_e is the expected proportion of agreement. The Kappa statistic typically ranges from between 0 and 1, with values closest to 1 reflecting highest agreement (Jenness and Wynnes, 2005). The Kappa coefficient was

measured for waterholes larger and smaller than the resolution of the Landsat image, to evaluate the effect of mixed pixels as a result of small waterholes (Ji et al., 2009). Based on the Kappa results, the MNDWI performed better than the SWI, thus the MNDWI was selected for further analysis. Due to unavailability of adequate high resolution imagery for validating MNDWI detected-waterholes from previous years, the waterholes were validated by assessing their relationship to rainfall from 1990 – 2016.

2.2.2.4 Spatial pattern of waterholes

Based on the established MNDWI threshold, waterhole presence for one dry season image for each year within the study period was classified and this resulted in a total of 19 yearly images. The spatial distribution of waterholes from classified MNDWI images was visually assessed in relation to temporal rainfall categories i.e. below-average, average and above-average rainfall years. The clustering of waterholes in relation to temporal rainfall patterns was further analysed using the G nearest neighbour distribution function (Ghat) (Rowlingson and Diggle, 1993). In the analysis, waterholes were represented by polygon centroids.

2.2.2.5 Rainfall data

TAMSAT (Tropical Applications of Meteorological Satellites) data were used as the source of spatial rainfall data. The TAMSAT data are quantitative estimates of rainfall made by local calibration of satellite data against rainfall measurements within climatically similar zones (Thorne et al., 2001). TAMSAT rainfall estimate data acquired on a 10-day basis and with a spatial resolution of 4km were downloaded for the period January 1983–July 2016. Satellite-derived rainfall was checked whether it matched with *in situ* rainfall measurements. In this

regard, data were first tested for normality using the Shapiro Wilk test. Results showed that satellite rainfall data did not conform to a normal distribution (p = 0.011), while the *in situ* rainfall measurements did not deviate from a normal distribution (p = 0.277). The non-parametric Spearman Rank correlation test was then used to assess whether satellite rainfall estimate data and *in situ* rainfall were significantly correlated. The Spearman rank correlation coefficient was used as it is more robust to outliers than the Pearson product-moment correlation coefficient (Nussbaum, 2014). The Spearman Rank correlation test showed that there was a statistically positive significant correlation (r = 0.758, p = 0.000) between TAMSAT rainfall estimates (rfe) and HNP rainfall data from 1984–2005. However a plot of the data shows that in some years, TAMSAT rainfall estimates tend to underestimate rainfall amount in relation to *in situ* rainfall measurements in HNP (Figure 2.2). Next, the TAMSAT rainfall estimates were used to perform temporal and spatial analysis of rainfall over the years. For integration with Landsat images, TAMSAT rainfall estimate images were resampled to 30m using the nearest neighbour method and re-projected to UTM zone 35 south projection and World Geodetic System 1984 datum.

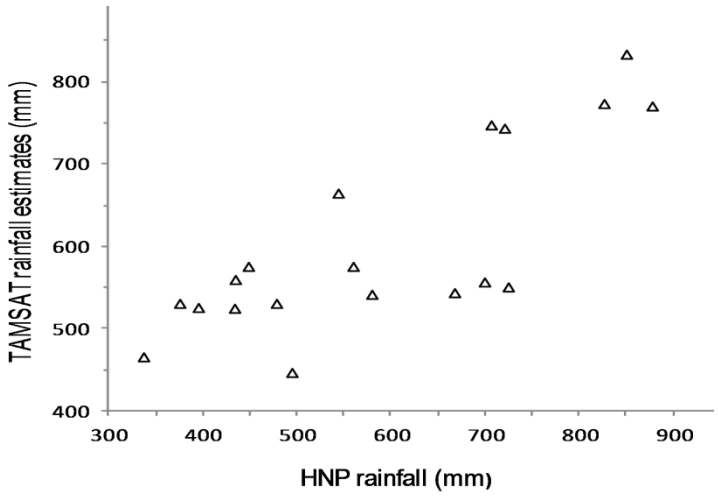

Figure 2.2 Significant (P < 0.05) correlation between satellite rainfall estimates and Hwange Main Camp rainfall measurements

2.2.3 Statistical analysis

2.2.3.1 Trend analysis

In order to test whether waterhole area increased or decreased monotonically over the years (1990–2016) the non-parametric Mann-Kendall trend test was used. With the Mann-Kendall trend test there are no distribution assumptions (Helsel and Hirsch, 1993). The basis of the Mann-Kendall test is to determine change of the median over time. From the 19 classified yearly MNDWI images pixels classified as water were extracted and also the area of the water pixels of each year was determined.

2.2.3.2 Waterhole area and annual temporal rainfall relationship

In order to determine whether waterhole area was linked to annual temporal rainfall pattern, polynomial regression analysis was performed. Prior to regression analysis, distribution of data was assessed using a scatter plot, which showed that pattern of data did not accurately conform to a linear fit.

2.2.3.3 Waterhole persistence and spatial rainfall relationship

Waterhole persistence was measured using images acquired on a monthly basis for the entire dry season for the period 1990–2016. For each waterhole, surface water presence and absence were recorded using binary coding for each month and water presence counts were averaged by the number of dry season months for when data were extracted. Waterhole persistence values had a range of 0–1. For each waterhole, pixel values of mean annual rainfall were extracted by overlaying the TAMSAT rainfall images with digitised waterhole mask. It was determined whether waterhole persistence varied in relation to spatial rainfall variability using Kruskal-Wallis test. Annual rainfall was categorised as above-average, average and

below-average for each year. Class breaks for above-average, average and below-average were placed above and below the mean annual rainfall at intervals of standard deviation where the interval size was 1std, based on the standard deviation classification method in ArcGIS 10.2 (ESRI, 2014).

2.3 Results

2.3.1 Optimal threshold for detecting waterholes using MNDWI in HNP

It can be observed that the probability of detecting waterholes using MNDWI is deemed optimal at -0.29 (Figure 2.3) and using SWI, -0.72 (Figure 2.4). Probability of detecting waterholes is higher using MNDWI than SWI at their optimal thresholds (Table 2.1). Detection of water from waterholes is better when excluding waterhole areas less than 2025m^2 as shown by the Kappa values of 0.85 and 0.24 for MNDWI and SWI respectively (Table 2.1). The proportion of waterhole area represented by waterholes less than 2025m^2 is 0.2.

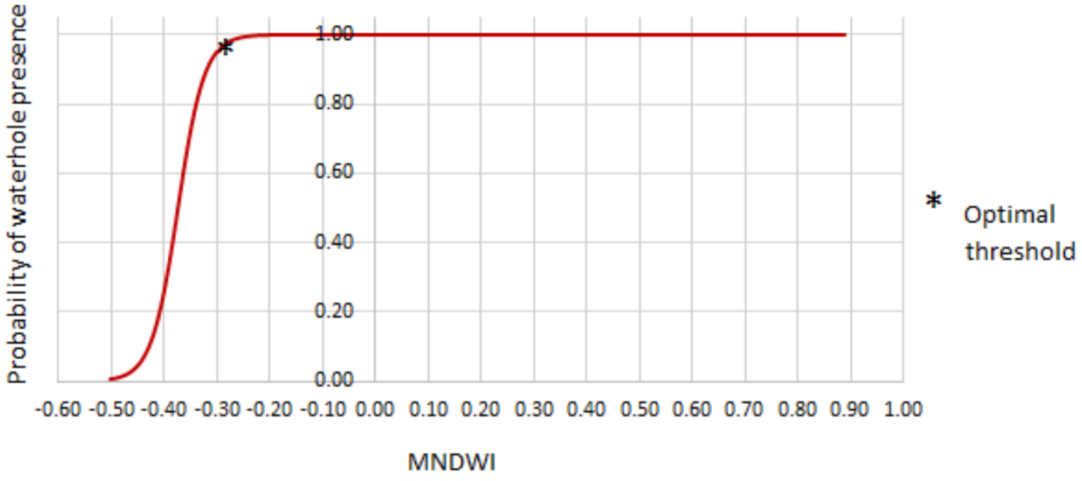

Figure 2.3 The probability of waterhole presence using MNDWI as determined using a binary logistic model

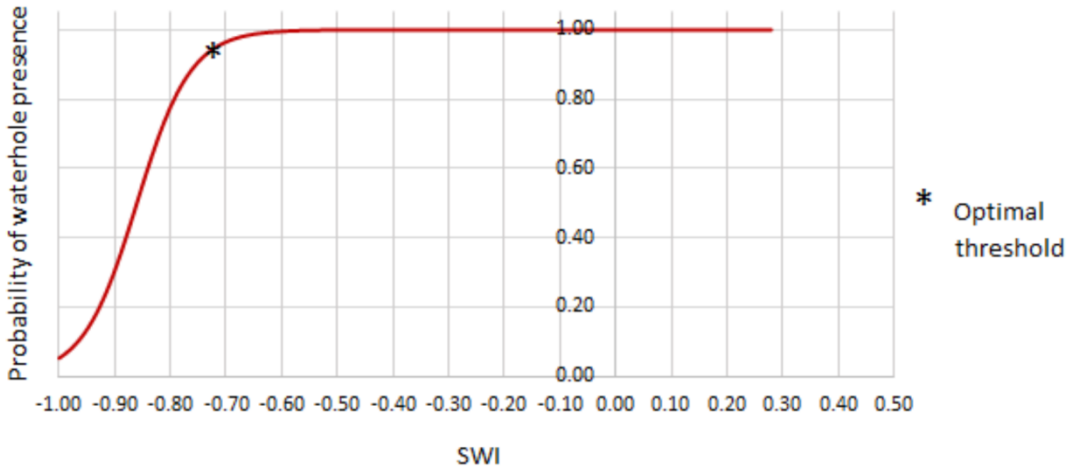

Figure 2.4 The probability of waterhole presence using SWI as determined using a binary logistic model

Table 2.1 Classification accuracy assessment

Water Index	***Optimal Threshold***	***Kappa coefficient***	
		including waterhole areas <2 025m^2	*excluding waterholes <2 025m^2*
MNDWI	-0.29	0.64	0.85
SWI	-0.72	0.14	0.24

2.3.2 Mapping waterholes using MNDWI in the dry season in HNP

Significant variations in the spatial distribution of waterholes can be observed during the dry season (Figure 2.5). Following a below average rainfall season, waterholes become more concentrated in the northen part of HNP with a few waterholes in the south central parts of HNP (Figure 2.5a and 2.5b). During an average rainfall season waterholes become widespread in a manner more pronounced than a below average rainfall season (Figure 2.5c and 2.5d). Next, in an above-average rainfall season, the dry season is characterised by widespread surface water availability in HNP (Figure 2.5e and 2.5f).

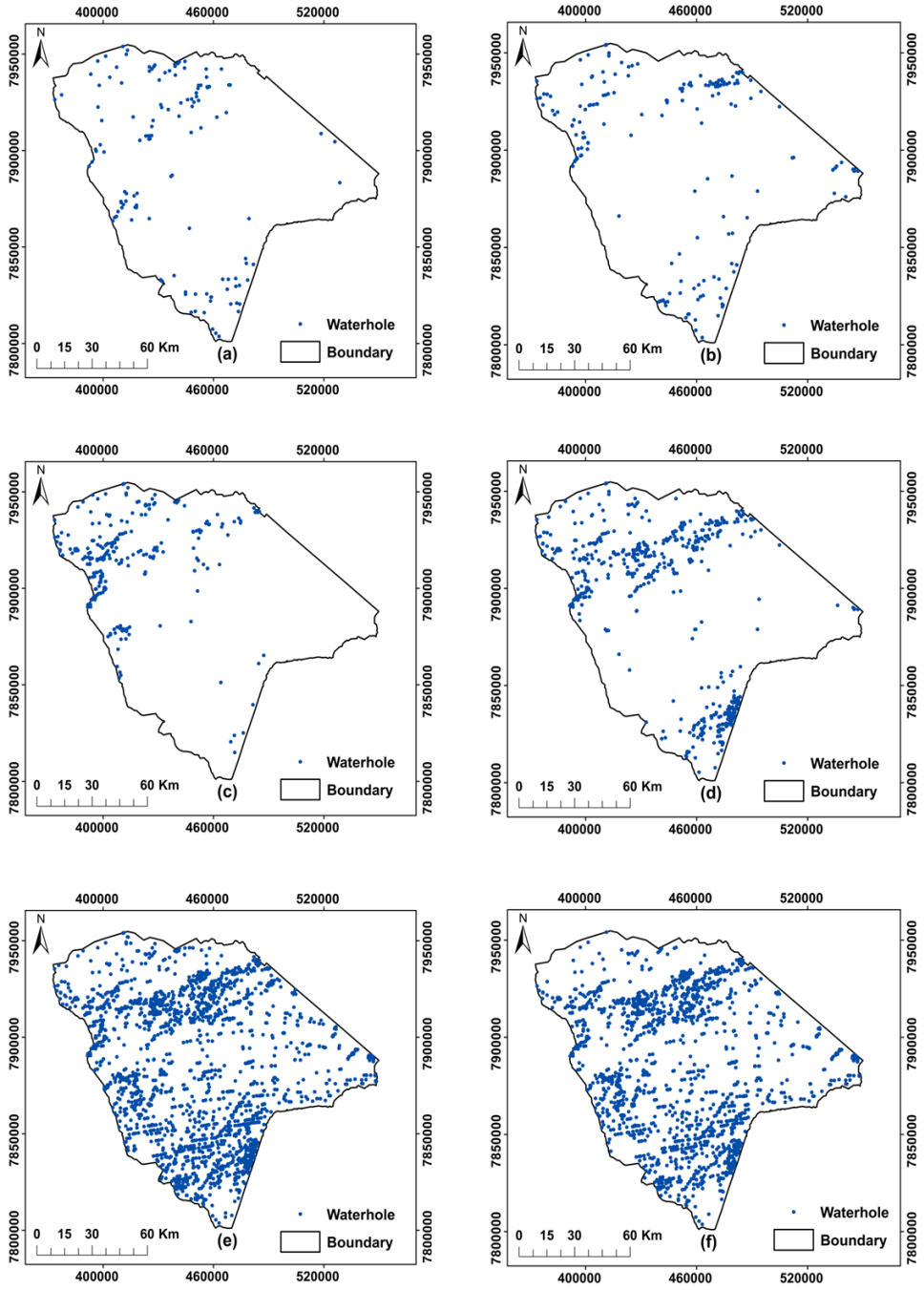

Figure 2.5 Dry season surface water distribution maps for below average rainfall years **a)** May 1995 (130 waterholes detected) **b)** May 2002 (176 waterholes detected); average rainfall years **c)** May 1992 (263 waterholes detected) **d)** June 2007 (505 waterholes detected); above-average rainfall years **e)** June 2004 (2001 waterholes detected) **f)** May 2006 (1593 waterholes detected). Map coordinates are in metres based on UTM zone 35 south, WGS 1984 spheroid

For the below average rainfall season, the Ghat function rises slowly for small distance (0.65 at 2500m). When there is average rainfall, there is intermediate increase of Ghat at small distance (0.85 at 2500m). For the above-average rainfall season, there is a rapid rise of Ghat for small distance (0.94 at 2500m) (Figure 2.6) indicating that waterhole distribution pattern becomes more clustered as annual rainfall increases.

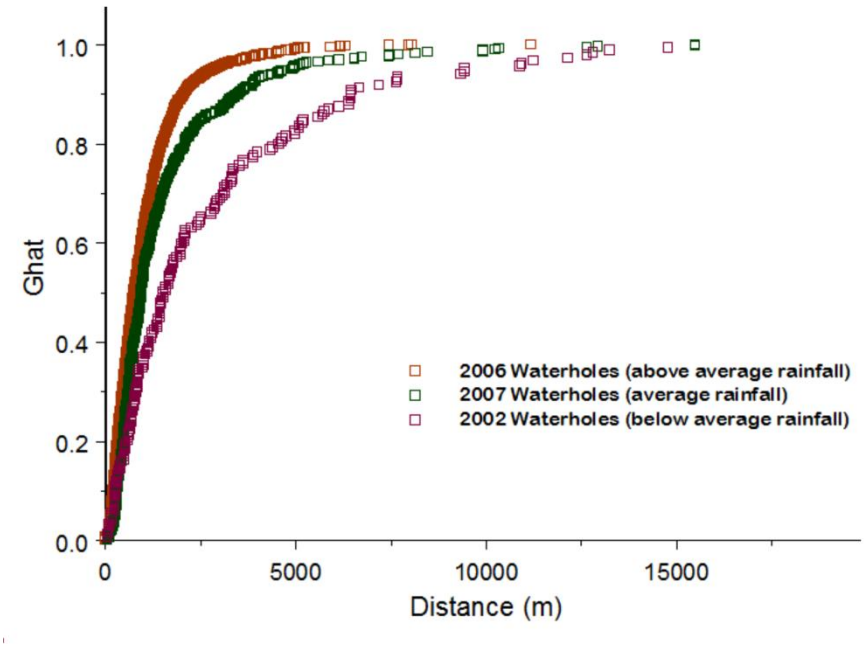

Figure 2.6 Spatial pattern analysis for above-average rainfall season waterholes (May 2006), average rainfall season waterholes (June 2007) and below-average rainfall season waterholes (May 2002)

2.3.3 Temporal variations in waterhole area

Based on trend analysis of waterhole area for the period 1990–2016, it can be observed that there is no significant temporal trend for surface water availability for the dry season (τ = 0.2515, p = 0.1417) (Figure 2.7).

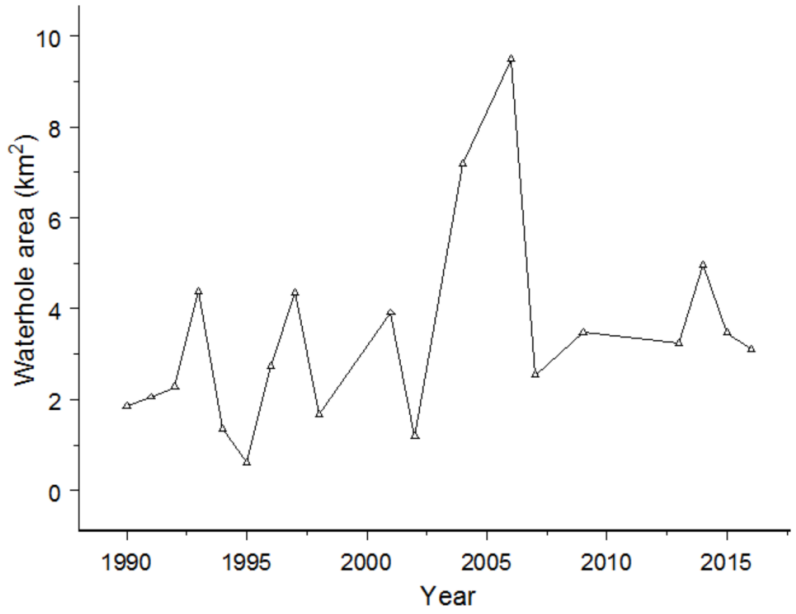

Figure 2.7 Time series for dry season waterhole area

2.3.4 Waterhole area in response to annual temporal rainfall patterns

Based on the quadratic regression model which fitted the data well, it is observed that there is a curvilinear relationship between annual temporal rainfall and waterhole area (Figure 2.8). It can be observed that an increase in annual temporal rainfall results in an increase in dry season waterhole area. Results show that annual temporal rainfall pattern significantly explains 87% of waterhole area variance in the dry season of each year (Table 2.2).

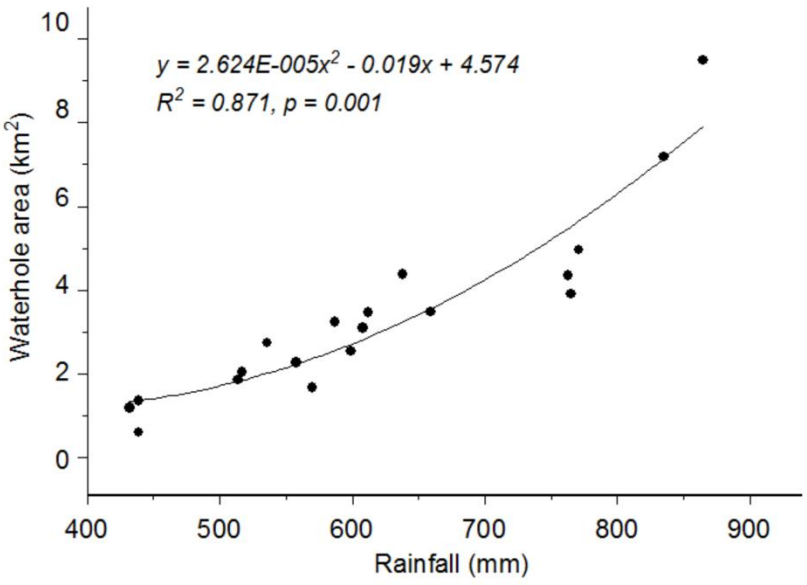

Figure 2.8 Quadratic model fit for annual temporal rainfall and waterhole area for the years: 1990; 1991; 1992; 1993; 1994; 1995; 1996; 1997; 1998; 2001; 2002; 2004; 2006; 2007; 2009; 2013; 2014; 2015 and 2016

2.3.5 Waterhole persistence in response to spatial rainfall variability

Waterhole persistence does not significantly differ due to spatial rainfall variability (χ^2 (2) = 1.594, p = 0.451) (Figure 2.9) in HNP.

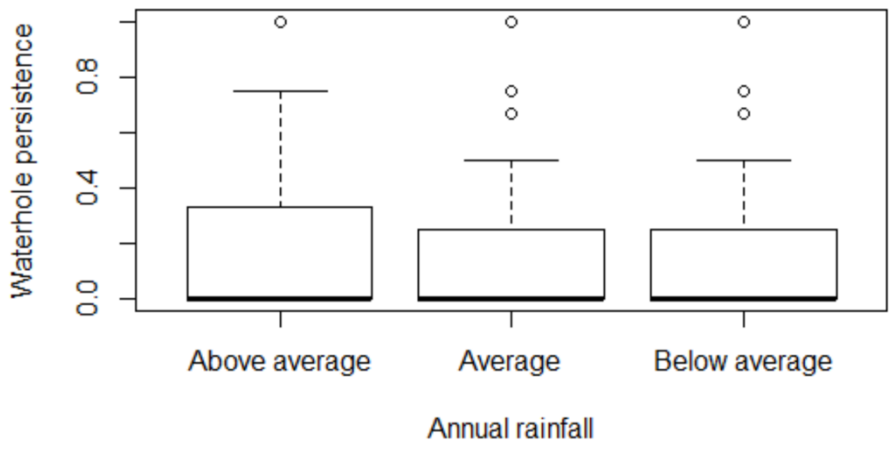

Figure 2.9 Boxplot of dry season waterhole persistence and spatial rainfall variability

2.4 Discussion

Results of this study show that MNDWI is the water index that better detects waterholes than SWI. Thus, it is deduced that MNDWI is more efficient at detecting waterholes which can be as small as 2025m^2 compared to the SWI (Table 2.1). From the results of this study, it can be further deduced that the threshold for detecting small surface water features such as waterholes can be adjusted for optimum agreement between remote sensing-based classification and high resolution imagery data or ground reference data. In this regard, results indicate that a threshold of -0.29 is the one suited to semi-arid ecosystems for detecting waterholes and that it best detects waterholes that are relatively larger than the pixel size of Landsat satellite imagery. Previous studies have mostly used a threshold of 0 and above 0 for detecting surface water but this has been mostly used to detect larger surface water features (Hui et al., 2008; Deus and Gloaguen, 2013; El-Asmar et al., 2013; Gautam et al., 2015). However, it is acknowledged that there is need to also test the consistency of the threshold at a different site experiencing similar conditions.

Results to validate existence of the remotely-sensed waterholes indicate that the remote sensing-based method used in this study to delineate waterholes, produced results that are consistent with previous studies done in HNP using ground survey methods, where interannual fluctuations in rainfall strongly affected natural surface water availability (Chamaillé-Jammes et al., 2007a). These findings are also consistent with those of Cronje et al., (2005) in Manyeleti Game Reserve, Gaylard et al., (2003) and Smit, (2013) in Kruger National Park and Kaptué et al., (2013) in the Sahel semi-arid region. Findings of these studies show that variation in surface water availability and distribution is strongly linked to temporal rainfall patterns. However, results to validate remotely-sensed waterholes using spatial rainfall data show that there is no significant variation in waterhole persistence as a

result of spatial rainfall variability. This is contrary to the expectation that above-average rainfall areas would result in high waterhole persistence or that below average rainfall areas would result in low waterhole persistence. In this study, characterisation of each remotely-sensed waterhole was not done given the large number of remotely-sensed natural waterholes that would have to be characterised. However, there is work that has been previously done to identify waterhole types based on field surveys in HNP (Chamaillè-Jammes et al., 2007a) and it was observed that natural water pans are the most sensitive to rainfall variations compared to other waterhole types. The result of this study where waterhole persistence was not related to spatial rainfall variability could be explained by the differences in these waterhole types i.e. pans or springs. For example, pans are directly fed by rainfall and are likely to respond linearly to rainfall fluctuations while springs may not behave similarly because they additionally rely on ground water. Thus, differences in waterhole type or merely low spatial rainfall variability, or other factors such as percolation due to differences in soil type, size of pans or animal activity could explain lack of disparities in waterhole persistence. Hence in this study, it can be deduced that waterholes can be better validated using temporal rainfall data than spatial rainfall data.

Waterhole mapping at the HNP scale reveals that there is strong evidence of spatio-temporal variation in distribution and availability of natural surface water as explained by the severity of the rainfall gradient from year to year. Results of waterhole configuration indicate that when there is below-average rainfall, water availability is low and waterholes are sparsely distributed in HNP. When there is average rainfall, water availability is intermediate with waterholes being concentrated in the north and south of the park. When there is above-average rainfall in HNP, water availability is high and is widely distributed across the park up to the end of the dry season. This is not only logical but also consistent with other findings in

Kruger National Park, South Africa, where above-average rainfall years result in a large number of persisting pools and below-average rainfall years resulted in only a few deeper river pools persisting through the end of the dry season (Gaylard et al., 2003). To further confirm our visual interpretation of waterhole configuration, spatial pattern analysis reveals an increase in clustering of waterholes at short distance in an above-average rainfall year, intermediate clustering of waterholes in an average rainfall year and less clustering in a below-average rainfall year. A snapshot of spatial variation in the distribution and availability of water at regular time intervals is important for the monitoring of water supply for wildlife especially during drought years.

Our results indicated that water availability varies from year to year without evidence of a significant trend and this is contrary to the speculation that surface water availability may be decreasing due to an increase in aridity in semi-arid regions of Africa (Shrader et al., 2010). These results are consistent with those of studies done in southern Africa, where over the past 50 years, the total annual rainfall, which has a direct effect on surface water availability, has shown neither decreasing nor increasing trend in a clear pattern but an increase in variability of rainfall between the years (Shanahan et al., 2013). For studies done in the semi-arid regions of Africa, all results to suggest a drying climate have not been statistically significant (Chamaillé-Jammes et al., 2007b). However, studies done in HNP show that dry years are becoming drier (Chamaillé-Jammes et al., 2007b), confirming the view of increased drought severity in arid and semi-arid regions.

This study is distinctive in testing the applicability of remotely-sensed water indices MNDWI and SWI in waterhole detection as well as the optimal threshold that could be most suited to

detecting waterholes in semi-arid areas. It can be concluded that MNDWI can efficiently be used to detect and map waterholes at an optimal threshold of -0.29. Understanding trends and distribution patterns of waterholes through the successful mapping of waterholes, is critical for the management of ecosystems. For example, surface water availability is regarded as a key driver of elephant impacts on biodiversity (Landman et al., 2012). To this end, this study provides a necessary preamble to the assessment of the effects of variation of surface water availability on wildlife population dynamics, as well as their possible effects on surrounding vegetation heterogeneity in semi-arid ecosystems.

The limitation of this study was the exclusion of a range of smaller waterholes (less than 2025m^2 in size) which could not be detected using Landsat images because of its medium spatial resolution (30m). It is recommended that further research is needed in identifying the spatial resolution of satellite imagery best suited to detecting the spectrum of smaller waterholes. The minimum size of waterholes that can be considered can at least be twice the pixel of the satellite remotely-sensed image. A combination of remotely-sensed data i.e. multispectral images and digital elevation models may also enhance detection of waterholes.

Chapter 3: Elephant-induced landscape heterogeneity change around artificial waterholes in a protected savanna woodland ecosystem

---

This chapter is based on a manuscript submitted to Remote Sensing Applications: Society and Environment: **Zorodzai Dzinotizei, Amon Murwira and Mhosisi Masocha**

Elephant-induced landscape heterogeneity change around artificial waterholes in a protected savanna woodland ecosystem

Abstract

In protected areas, establishment of artificial waterholes has been hypothesised to result in increased elephant *(Loxodonta africana)* densities around these waterholes which would in turn result in changes in landscape heterogeneity. To test this hypothesis this study first assessed the relationship between waterhole distribution from remotely-sensed waterholes and elephant density in Hwange National Park (HNP), Zimbabwe. The study tested using the coefficient of variation of the Normalised Difference Vegetation Index (NDVI CoV) the short-term effects of varying elephant densities on vegetation heterogeneity change at the landscape scale. This study also tested the relation between artificial waterholes and surrounding landscape heterogeneity change. In addition the study assessed the potential influence of spatial variability in rainfall on landscape heterogeneity change. Landscape heterogeneity change was assessed using the landcover maps for the years 1990 and 2016 based on the post classification method. The landscape metrics: mean patch size; patch density; class area and mean nearest neighbour distance were used to measure landscape heterogeneity. Results indicate that elephant density in HNP increases in response to the increase in concentration of late dry season waterholes. Results indicate that there is no relationship between elephant density and vegetation heterogeneity change at the seasonal scale (short-term). This could be attributable to differences in sensitivity and response of different vegetation types to elephant browsing even the variable foraging preferences of elephants at the landscape scale regardless of elephant occupation. Findings of this study imply that in the long term, maintenance of artificial waterholes results in a decrease in woody vegetation structural heterogeneity through conversion of woodlands to coppiced bushland in areas with high artificial waterhole density. Findings of this study also show that landscape heterogeneity change is not being considerably influenced by the existing north-east to south-west gradient of decreasing rainfall in HNP.

3.1 Introduction

African elephants *(Loxodonta africana)* modify the savanna landscape due to the way they feed, that is, by toppling trees and breaking tree branches, (Hiscocks, 1999; Balfour et al., 2007; Kerley et al., 2008; Seloana et al., 2017). Thus, at high densities, elephants could alter woody vegetation structure by reducing tree density, transforming trees to short dense shrubs and decreasing overall woody vegetation structural diversity, resulting in a changed landscape configuration and composition (Trollope et al., 1998; Whyte et al., 2003; Holdo et al., 2009; Fullman and Bunting, 2014; Guldemond et al., 2017). In water-limited savanna ecosystems of southern Africa, the adoption and implementation of water provision policies has facilitated pumping of borehole water in pans to buffer shortages of natural surface water availability (Freitag-Ronaldson and Foxcroft, 2003). Previous research done in Hwange National Park, Zimbabwe has reported that the introduction of these artificial waterholes to satisfy wildlife watering needs particularly during drought years has triggered localised increases in elephant densities (Chamaillé-Jammes et al., 2007c). Research suggests elephant densities can be controlled through surface water management for regulating landscape heterogeneity (Chamaillé-Jammes et al., 2007c, 2016). However, to date, not much is known about the effects of varying elephant densities on magnitude of landscape heterogeneity change. Thus, the proper quantification of the effects of elephant densities on woody vegetation structure based on cost-effective methods such as remote sensing is critical for managing protected areas in light of changes in function related to provision of artificial waterholes.

The development of satellite remote sensing and GIS technology has provided an opportunity to quantify changes in landscape heterogeneity at fine spatial and temporal resolutions as well

as at large spatial extents and in the long term (O'Neill et al., 1999; Rogan and Chen, 2004; Fichera et al., 2012). Application of this technology also provides an opportunity for scientists to better understand elephant density effects on landscape heterogeneity in areas with artificial waterholes. Several studies have quantified effects of elephants on changes in woody vegetation For instance Dublin (1995) used aerial photographs to describe changes in woody vegetation cover and field experimental work to quantify annual rates of tree damage and mortality caused by elephants. Skarpe et al. (2004) used field assessments on woody vegetation change and use by elephants in permanent sample sites. Brits et al. (2002) used field assessments to quantify woody vegetation and composition change in an area with high elephant densities. Mosugelo et al. (2002) used aerial photographs and field surveys to assess elephant browsing impact in different vegetation types. Teren and Owen-Smith (2010) used field surveys to assess tree mortality, sapling abundance and extent of shrub cover in evaluating the role of elephants in riparian woodland change. However, these studies have mainly been based on time and cost intensive field-based methods and aerial photographs hence these were largely conducted either on small spatial extents or over widely spaced temporal intervals. The quantification of the impacts of different elephant densities on landscape heterogeneity based on satellite remotely-sensed data is still rudimentary yet it is critical for understanding impacts of human intervention on savanna ecosystems.

This study tested the relationship between waterhole distribution, mapped using a remote sensing water index and elephant density in the late dry season, based on data from Hwange National Park (HNP) in Zimbabwe. Short term (seasonal scale) satellite remotely sensed data with elephant density data from aerial surveys were used to test whether varying elephant densities in the short term have significant effects on vegetation heterogeneity change at the landscape scale. Land cover maps were used with artificial waterhole density data from

ground surveys to test whether different landscape configuration and composition evolve as a result of artificial waterholes in the long term. In addition, the influence of spatial variability in rainfall on landscape heterogeneity change was also evaluated, where mean annual precipitation is a major driver of woody cover dynamics in semi-arid savanna ecosystems (Sankaran et al., 2005).

3.2 Materials and methods

3.2.1 Study site

The study area is Hwange National Park (HNP) which lies between latitudes 18° and 20° S and longitudes 25, 4° and 27, 4° E in North West of Zimbabwe (Fig 3.1). The park is 14 651km^2 in area and is subdivided into 11 management blocks. The park has one of the highest elephant densities in Africa with an average elephant density of 3 elephants/ km^2 (Chamaillé-Jammes et al., 2009b) but there is variability in the spatial distribution of elephants across the park. The northern blocks comprising the Main Camp and Shapi sustain the highest elephant density of 9 elephants/km^2 in the late dry season in some years while the southern block Shakwanki sustains the lowest elephant density with densities of <0.5 elephants/ km^2 having been recorded (Chamaillé-Jammes et al., 2009b; Davies, 1996). Interspersed among artificial waterholes are hundreds of natural waterholes of varying sizes which are mostly ephemeral and dry out as the dry season progresses.

The climate is semi-arid, characterised by low and erratic rainfall which varies between 300 and 800mm per annum. The wet season is typically short, from November to March and the dry season is long, from April to November, with mean annual temperatures between 20 and 30°C. The soil is dominated by Kalahari sand supporting woodland communities dominated by *Combretum spp, Colophospermum mopane* and *Baikiaea plurijuga.* The bushland communities are more diverse and are made up of a mix of *Terminalia sericea, Burkea africana, Ochna pulchra, Baphia massaensis* among other species (Rogers, 1993). Woody vegetation is interspaced by patches of grassland.

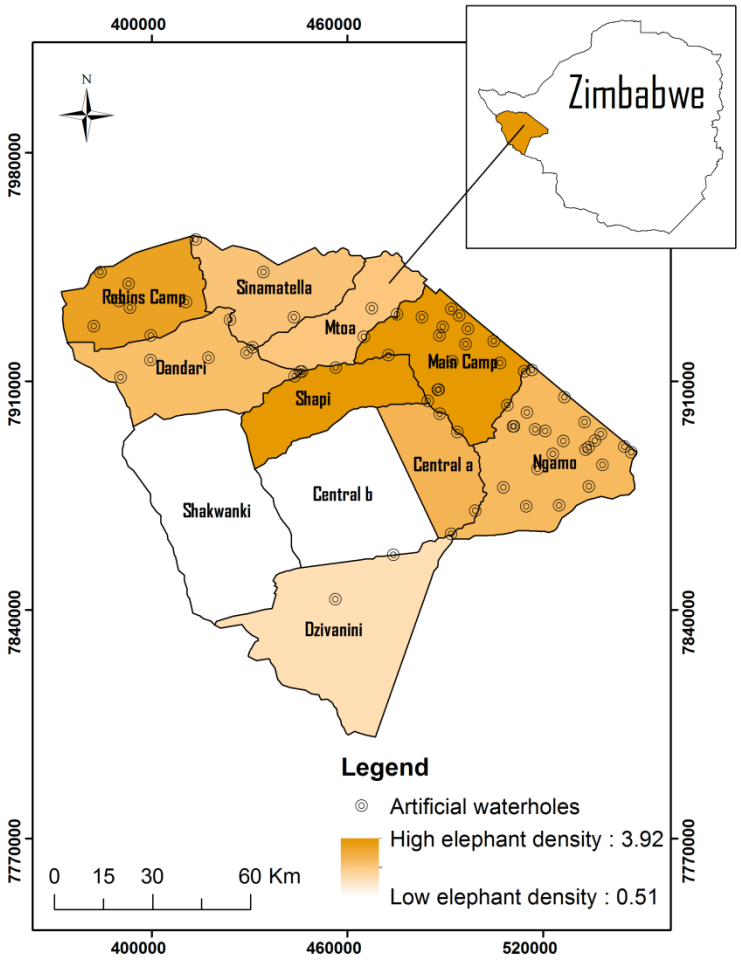

Figure 3.10 Map of Hwange National Park showing spatial variability of mean elephant density and artificial waterhole distribution in eleven management blocks. Map coordinates are in metres based on UTM zone 35 south, WGS 1984 spheroid

3.2.2 Remotely- sensed data and methods

3.2.2.1. Image pre-processing

Landsat 5 TM (Thematic Mapper), Landsat 7 ETM+ (Enhanced Thematic Mapper) and Landsat 8 OLI (Operational Land Imager) images were downloaded from www.usgs.gov for the early dry season (April–July) and late dry season (late August–October) for the years:

1990, 1992, 1993, 1994, 1995, 2001, 2007, 2014 and 2016. To cover the study area three Landsat scenes (Path/Row 172/73, 173/73 and 172/74) with dates of image capture being as close as possible were used. For the early dry season of the year 2001 August images were used since images for the period April–July for that year were not all available. For the year 2007, in the late dry season only two Landsat scenes were used (Path/Row 172/73 and 172/74), the (173/73) scene was not available. Landsat TM, ETM+ and OLI images were used as their spatial resolution (30m) is fine and suitable for analysis of vegetation response to spatial variability of elephant distribution at the landscape scale (Shrader et al., 2012). Due to inaccessibility of some areas covered by the image scenes in our study area, a minimum of 15 ground control points (GCPs) per image scene which included road intersections were collected from high resolution imagery made available through Google Earth (www.googleearth.com). The GCPs were used to geometrically correct the 2016 Landsat image. The nearest neighbour technique was used to resample the image and a root mean square error less than 0.5 was achieved. Image co-registration for images from previous years was done using the geometrically registered 2016 Landsat 8 OLI image scenes. Radiometric correction was done using ENVI 5.1 (ITT, 2013) by converting Digital Numbers (DNs) to Top-of-Atmosphere Reflectance. This correction is important for reducing between scene variability due to sensor differences; Earth-sun distance and solar zenith angle (Bruce and Hilbert, 2006) so that image scenes from different Landsat sensors and acquisition dates are comparable (Chander and Markham, 2003).

3.2.2.2 Mapping vegetation heterogeneity from remotely sensed image spectral heterogeneity

The spectral variation hypothesis proposes that the spectral heterogeneity of a remotely sensed image is correlated with landscape structure and complexity which reflects

heterogeneity of the habitat (Oldeland et al., 2010). The coefficient of variation is a simple measure of spectral heterogeneity (Rocchini et al., 2010) and coefficient of variation of NDVI (NDVI CoV) has been successfully used as an index for assessing spatial variability in vegetation cover (Oindo and Skidmore, 2002) and detecting selectively logged areas in dry savannas (Mapfumo et al., 2017). CoV using NIR reflectance band in combination with Soil Adjusted Vegetation Index (SAVI) have also been used in predicting tree species diversity (Mutowo and Murwira, 2012). Therefore the NDVI CoV was used as a proxy for vegetation heterogeneity to assess the effects of elephant densities on changes in vegetation cover and structure through branch breaking, tree toppling, and browsing by elephants from the early dry season to the late dry season of each year for the years 1990, 1992, 1993, 1994, 1995, 2001, 2007 and 2014. NDVI CoV for the early dry season was subtracted from the NDVI CoV in the late dry season of each year to assess the magnitude of change in spatial variability of vegetation cover and structure in relation to different elephant densities across the landscape in the dry season. NDVI was initially calculated using the Near Infrared (NIR) spectral band such as TM band 4, ETM+ band 4, OLI band 5 and the red spectral band such as TM band 3, ETM+ band 3 and OLI band 4. The vegetation index was calculated using the ratio:

$$NDVI = \frac{NIR - Red}{NIR + Red}$$

Equation 4

Where NDVI measures vegetation greenness and photosynthetic activity (Walker et al., 2012). NIR is the band which measures reflectance in the near infrared wavelength range. Red is the band which measures reflectance in the red wavelength range. Green vegetation absorbs most of the red light and reflects a large portion of

near infrared radiation. Calculation of NDVI will result in a range of -1 to +1. Where zero indicates no vegetation and close to +1 indicates the highest density of green vegetation.

NDVI CoV was then calculated from the standard deviation *(σ)* of NDVI and mean *(μ)* NDVI using a neighbourhood filter of 3*3 pixels as follows:

$$NDVI\ CoV = \frac{\sigma}{\mu}$$

Equation 5

Where NDVI CoV measures pixel level NDVI variation (Weiss and Milich, 1997). σ is the standard deviation (measure of dispersion from the mean) of NDVI pixel values and μ is the mean (average) of NDVI pixel values.

3.2.2.3 Mapping land cover types using remotely-sensed data

To map land cover types ground data on land cover was initially collected in the field in HNP for the early dry season of June 2015 when vegetation cover classes can be better distinguished from satellite imagery (Weiss et al., 2004). Transects were randomly selected using Arcview 3.2 (ESRI, 2002) within the Main Camp and Ngamo area in HNP for ease of accessibility. Transects radiated from 25 waterholes and were 1 km long. The basis for location of sampling transects was that around waterholes there would be high variation of vegetation types at short distances. Sample plots 45*45m in size were demarcated at every 200m interval along a transect. In the field each transect was navigated by a handheld GPS, in all 142 plots were sampled. In each sampling plot, the geographic coordinates of the centre of the plot were captured and data on the proportion of area covered by each vegetation type/land cover were recorded based on the visual estimation method. Four broad land cover

types were identified in the field: Bare ground, Grassland, Bushland and Woodland. The broad land cover type assigned to each sampling plot was based on the dominant vegetation/land cover type. When one or more vegetation/land cover strata (bare ground, grasses, bushes and trees) covered more than 20% of the plot area, the land cover type with more than 20% forming the uppermost strata layer was assigned the dominant layer/broad land cover class (FGDC, 1997; Rogers, 1993) as shown (Table 3.1). The vegetation cover composition classification adopted in this study was to ensure that the vegetation class differences were optimal based on the 30m spatial resolution of Landsat imagery used in this study.

Plots from field work in 2015 were overlaid on high resolution images made available through Google Earth (www.googleearth.com). The high resolution images available which covered the study area and closely coincided with dates of field work were for the years 2016 and 2013. For landscape scale mapping using Landsat images, larger plot areas of homogeneous land cover were then digitised at the field plot locations and more sample plots in less accessible areas in HNP were also digitised. From historical high resolution images made available through Google Earth (for the years 1989 and 1990), sampling areas representing the different land cover classes identified in the study area were digitised. Additional land cover areas that could be easily distinguished from false colour composite Landsat images for the years 1990 and 2016 were also digitised. Digitised areas from high resolution imagery were sub sampled to areas of 3*3 pixels based on the spatial resolution of Landsat imagery. The 3*3 pixel dimensions were deemed suitable to allow linking to Landsat pixels while accommodating for registration errors and minimising the salt and pepper pixel effect (Knight and Lunetta, 2003; McCoy, 2005; Rutchey and Godin, 2009). The year 1990 had 240 sample plots and the year 2016 had 252 sample plots. For each year 70% of the

sample plots were used as training data for image classification while 30% of the sample plots were withheld and used as test data for validating accuracy of the land cover classification. The Supervised classification using the Maximum likelihood classifier was applied to Landsat images (TM) for the year 1990 and (8 OLI) for the year 2016. For image cleaning a 3*3 pixel smooth filter was applied to remove salt and pepper pixels. Using 30% of the withheld test data, accuracy of the supervised classification for land cover (Fig 3.2) was validated. Classification yielded an overall accuracy of 89.1% and a Kappa coefficient of 0.85 for the year 1990 and an overall accuracy of 88.1% and a Kappa coefficient of 0.84 for the year 2016.

Table 2.1 Land cover type description adopted from Rogers (1993)

Land cover type	**Description**
Bare ground	bare ground cover >20%; grass, shrub or tree cover <20%
Grassland	dominant grass cover >20%; herbs and scattered woody vegetation cover <20%
Bushland	shrubs <3m are dominant; bush canopy cover >20%
Woodland	trees >3m are dominant; open or continuous; tree canopy cover >20%

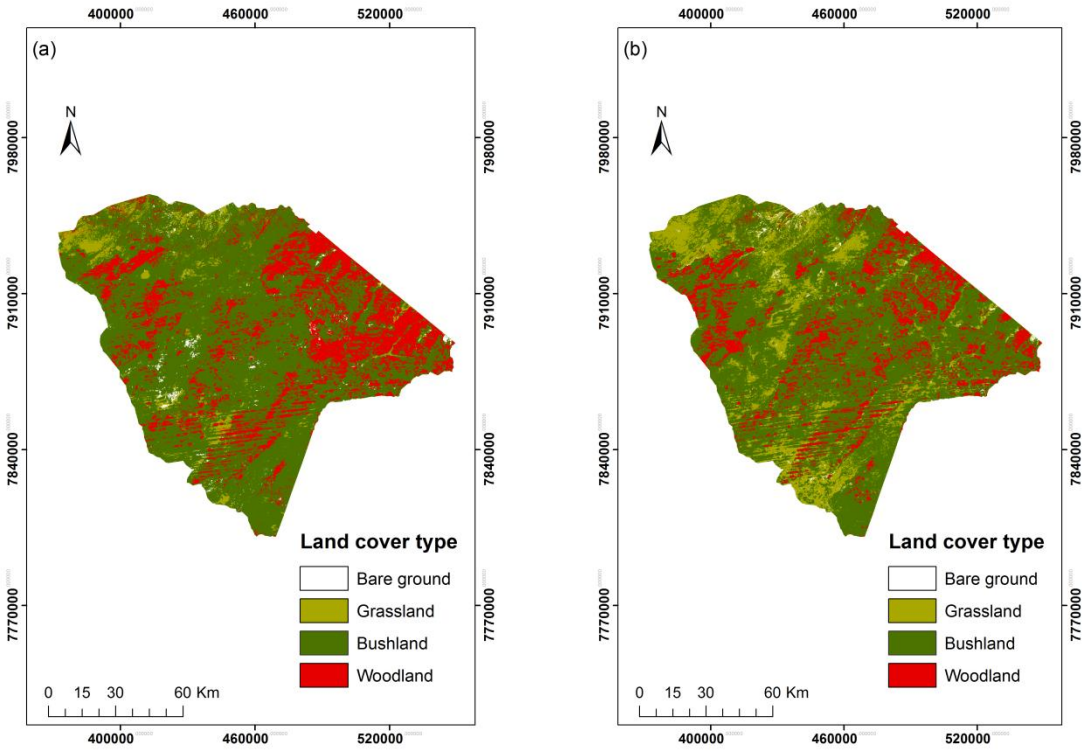

Figure 3.2 Classified land cover maps for Hwange National Park for (a) 1990 and (b) 2016 Map coordinates are in metres based on UTM zone 35 south, WGS 1984 spheroid

3.2.2.4 Landscape heterogeneity quantification

To determine the pattern and extent of landscape heterogeneity change landscape metrics were computed from the classified land cover maps, using Patch Analyst extension (Rempel and Carr, 2003) in Arcview GIS 3.2 (ESRI, 2002). Mean patch size, patch density, class area and mean nearest neighbour distance were the selected landscape metrics. Patch density was defined as the number of patches of each patch type in each landscape unit, mean patch size as the average area of each patch type in a landscape mosaic (units are in hectares), mean nearest neighbour distance as the average distance between patches to the nearest neighbouring patch of the same type (units are in meters) and class area as the total area comprised by each patch type (units in hectares) (McGarigal and Marks, 1995). Class area

was converted to class proportion to accommodate differences in area covered by each management block. Class proportion quantifies landscape composition, while mean patch size, patch density and the mean nearest neighbour distance are considered as metrics for landscape configuration (McGarigal and Marks, 1995). Patch density and mean nearest neighbour distance are also considered good indicators of the extent to which the landscape is fragmented (Eiden et al., 2000). The choice of landscape metrics was based on the metrics that can be well interpreted and related to change in landscape structure over time for instance the patch size decreasing or increasing over time.

3.2.2.5 Surface water detection

To identify waterholes which were holding water in the late dry season, Landsat images for the late dry season (late August–October) were used, which closely coincided with when aerial surveys for elephant counts were done. Cloud free images for the late dry season of 1991 were not available so this year was excluded from analysis. To map surface water, the Modified Normalised Difference Water Index (MNDWI) (Xu, 2006) was used. The MNDWI has been found to be more robust in delineating surface water (Li et al., 2013; Singh et al., 2015). The MNDWI was calculated using the Green spectral band such as TM band 2, ETM+ band 2, OLI band 3 and the middle infrared MIR spectral band such as TM band 5, ETM+ band 5 or OLI shortwave infrared spectral band SWIR band 6. The MNDWI was computed as:

$$MNDWI = \frac{Green - MIR}{Green + MIR}$$

Equation 6

Where MNDWI is the index which detects open water features (Xu, 2006). Green is the band which measures reflectance in the green wavelength range. MIR is the band which measures reflectance in the middle infrared wavelength range. Water absorbs most of the middle infrared radiation and reflects a large portion of the green light. This spectral water index gives a range of pixel values of -1 to 1, at the predefined threshold of 0, water is represented by the positive pixels while the negative pixels represent the non-water background, however the threshold can be adjusted for optimum agreement between image data and reference data (Xu, 2006). To delineate surface water from the non-water background, firstly all visible waterhole areas, river pools which remain after the ephemeral rivers have dried up in the dry season and depressions that could in time collect water and function as surface water sources were manually digitised from high resolution imagery made available through Google Earth (www.googleearth.com). The digitising procedure was done to mask out the non-water background whose spectral reflectance in spectral transformations is often confused with that of water, thereby overestimating surface water (Bochow et al., 2012; Du et al., 2012; Nigro et al., 2014; Verpoorter et al., 2012). Using high resolution imagery made available through Google Earth, data on water presence and water absence was collected from within the digitised water feature boundaries and used to determine an optimum threshold: which was found to be -0.29, (Dzinotizei et al., 2017). The -0.29 threshold was used for binary classification of MNDWI images, pixels above the optimal threshold were defined as water while those below the optimal threshold were defined as non-water. Surface water features which had an area greater than the pixel size of Landsat images (>2025m^2) were used in this study. The 2025m^2 area was regarded as suitable minimum size for detecting small surface water features such as waterholes while reliably linking to scale the water features to

the 900m^2 pixel dimensions of Landsat images, classification accuracy using waterhole areas >2025m^2 had a Kappa coefficient of 0.85 (Dzinotizei et al., 2017).

3.2.2.6 Elephant density data

Elephant density data were acquired from Zimbabwe Parks and Wildlife Management Authority (ZPWMA), data were from aerial survey reports of elephant counts done in HNP. The aerial surveys for elephant counts were carried out by ZPWMA and Non-Governmental Agencies in partnership with ZPWMA. Aerial surveys were done in the late dry season and sampling was based on the systematic random transect method and standard procedures were followed as prescribed by Norton and Griffiths (1978). Sampling intensity varied, in areas where there were expected to be high elephant densities, sampling intensity was higher than areas were elephant densities were expected to be low. Sampling was done in each of Hwange National Park 11 blocks i.e. Central A, Central B, Main Camp, Ngamo, Sinamatella, Shakwanki, Dzivanini, Robins Camp, Mtoa, Shapi and Dandari that are demarcated as shown in the Map of Hwange National Park (Fig 3.1).

Elephant density data used in this study was aggregated to management block units i.e. number of elephants per management block and analysis involving elephant density was conducted at this spatial scale. Data available were for nine years: 1990, 1991, 1992, 1993, 1994, 1995, 2001, 2007, and 2014. For the years 2000, 2002–2005 and 2008–2013 no aerial surveys were done and for 2006 the aerial survey was not completed due to technical problems with the plane. For the year 1991 there were no cloud free Landsat images available for the late dry season (late August–October), so this year was excluded from analysis. Late dry season elephant density for a given year was matched with MNDWI waterhole density

data for the late dry season to determine the influence of waterhole distribution on elephant densities across the landscape. NDVI CoV change data for the dry season was related with late dry elephant densities in order to assess the short-term (i.e. seasonal) effects of different elephant densities on vegetation heterogeneity change. The zonal statistics tool in ArcGIS 10.2 (ESRI, 2014) was used to integrate NDVI CoV change data and elephant density data for each stratum.

3.2.2.7 Artificial waterhole data

Artificial waterhole data were acquired from a spatial database of artificial waterholes in HNP, in all the park has ~69 artificial waterholes these were mostly established pre-1990 and were used for analysis in this study. Artificial waterhole density was calculated for each management block, i.e. number of waterholes per management block and analysis involving artificial waterhole density was also conducted at this spatial scale. Main Camp, Ngamo and Robins Camp have a high density of artificial waterholes hence elephant densities were expected to be high in the dry season for the long term. In contrast, Shakwanki, Central A and B and Dzivanini have a low density of artificial waterholes hence elephant densities were expected to be the low in the dry season for the long term. To assess the long term effects of elephant densities due to artificial waterholes on landscape heterogeneity change land cover maps for two dates: 1990 and 2016 were used to detect the changes based on the post classification method using landscape metrics.

3.2.2.8 Climatic variables

3.2.2.8.1 Spatial rainfall data

TAMSAT rainfall estimate data with ~4 km spatial resolution and a 10-day temporal resolution were used to map the spatial variability in rainfall in HNP. The TAMSAT algorithm of estimating rainfall uses a thermal infrared imagery to measure the length of time a satellite pixel is colder than a given temperature threshold which is then related to rainfall rate at the surface from rain gauge data (Asadullah et al., 2008; Gebremichael and Hossain, 2010; Thorne et al., 2001). The main advantage of TAMSAT data is the rainfall estimates are calibrated using local rain gauge data (Gebremichael and Hossain, 2010). TAMSAT rainfall data were combined for each year and the yearly rainfall images from 1990–2016 were used to compute the long-term average rainfall image for HNP. The rainfall image was resampled to 30m and projected to zone 35 south projection and World Geodetic System 1984 datum. The spatial rainfall image was classified into eight classes based on standard deviation from the mean; the classified image was comprised of forty polygons representing the eight standard deviation classes, the number of these polygons was the size of the samples used in this analysis. Fig 3.3 shows the north-west to south-east gradient of decreasing rainfall.

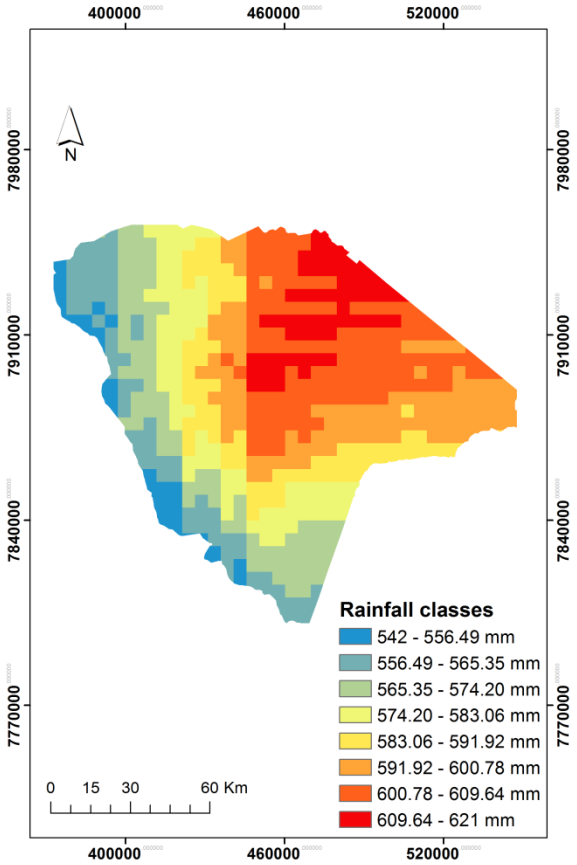

Figure 3.3 Classified rainfall map showing long term spatial rainfall variability in HNP. Map coordinates are in metres based on UTM zone 35 south, WGS 1984 spheroid

3.2.3 Statistical analysis

3.2.3.1 Spatial autocorrelation

Prior to statistical analysis data were tested for spatial autocorrelation using the Moran's I and Lagrange Multiplier coefficients computed using GeoDa software (Anselin, 2006). Spatial weights for the areal data were based on queen contiguity method (Anselin et al., 2006) where areas sharing the same boundary were considered to likely have an influence on another due to their close geographical placement. If the Moran's I was significant but neither the Lagrange Multiplier test for spatial lag and spatial error autocorrelation were significant,

the null hypothesis of spatial autocorrelation was rejected and non-spatial statistical methods were then used (Mariani and Fauzi, 2017). If either one or two of the spatial dependence model tests for Spatial Autoregression (SAR) and Spatial Error (SEM) were significant, the model with lowest p-value was then selected (Mariani and Fauzi, 2017).

3.2.3.2 Correlation between elephant density and waterhole density at landscape scale

Data were tested for normality using the Shapiro Wilk test prior to statistical analysis. The relationship between elephant density and waterhole density in each of the 11 management blocks was tested using the Spearman Rank correlation test since the data did not conform to a normal distribution ($p < 0.05$).

3.2.3.3 Relationship between elephant density and vegetation heterogeneity change in the short term

Prior to correlation analysis, data were tested for normality using the Shapiro Wilk test. Correlation analysis was used to test the short term effect of different elephant densities on vegetation heterogeneity change. Specifically, the Spearman Rank correlation analysis was used to test whether variability in elephant density within management blocks in the late dry season of a particular year is significantly related with magnitude of change in vegetation heterogeneity from the early dry season to the late dry season of that year.

3.2.3.4 Landscape heterogeneity change in relation to artificial waterhole density and spatial rainfall variability

Ordinary Least Squares Regression and Spatial Autoregressive Models were used to test for effects of artificial waterhole densities and spatial rainfall variability on land cover mean patch size, patch density, mean nearest neighbour distance and class proportion change.

3.3 Results

3.3.1 Correlation between elephant density and waterhole density at the landscape scale

Elephant density (elephants/km^2) was significantly and positively correlated with the density of remotely-sensed waterholes (waterholes/km^2) i.e. surface water sources available in the late dry season (r_s = 0.559, p = 0.001) (Fig 3.4).

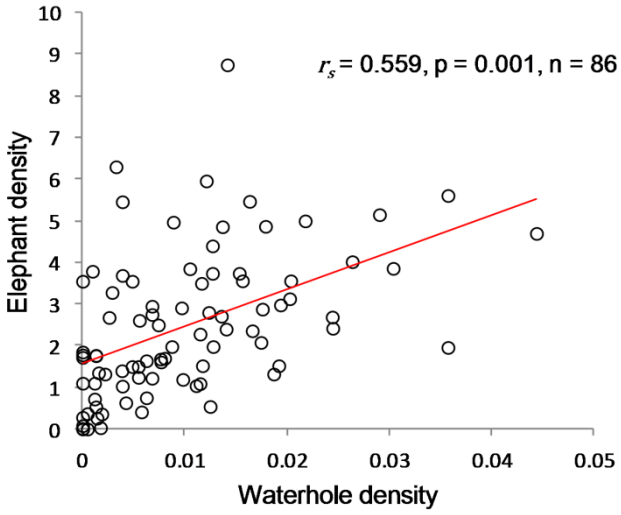

Figure 3.4 Correlation between elephant density and waterhole density is significant (P < 0.05)

3.3.2 Relationship between elephant density and vegetation heterogeneity in the short term

It can be observed that there is no statistically significant relationship between elephant density and vegetation heterogeneity change in the short term (r_s = -0.155, p = 0.153) (Fig 3.5).

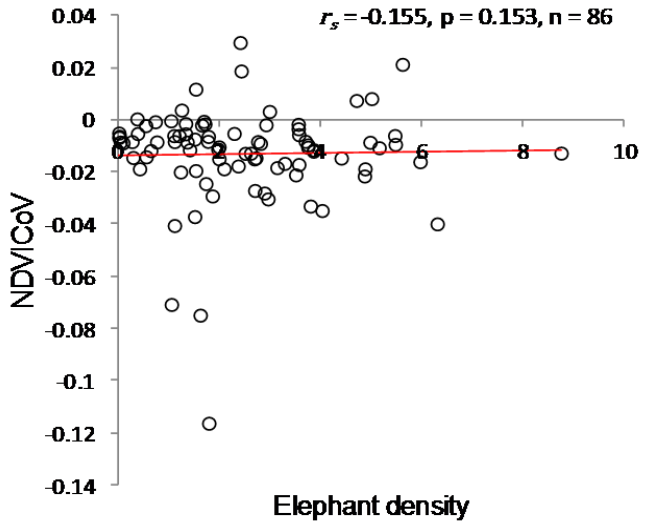

Figure 3.5 Relationship between elephant density and NDVI CoV is not significant (P > 0.05)

3.3.3 Landscape heterogeneity change in relation to artificial waterhole density

Table 3.2 illustrates that there are significant relationships between density of artificial waterholes and landscape metric change for different land cover types. It can be observed there is a significant positive relationship between artificial waterhole density and bushland mean patch size change (R^2 = 0.425, p = 0.03) and class proportion change (R^2 = 0.49, p = 0.016) while there is a statistically significant negative relationship between artificial waterhole density and bushland patch density change (R^2 = 0.441, p = 0.026). Results also show that there is a statistically negative relationship between artificial waterhole density and woodland mean patch size change (R^2 = 0.564, p = 0.008) and woodland class proportion change (R^2 = 0.68, p = 0.003).

.

Table 3.2: Ordinary Least Square (OLS) regression results for the relationship between artificial waterhole density and Mean Patch Size (MPS), Patch Density (PD), Mean Nearest Neighbour Distance (MNN) and Class Proportion (CP)

Land Cover Type	Landscape Metrics	Coefficient	R^2	p-value
Grassland	MPS	-0.00031	0.2138	0.1522
	PD	-0.00023	0.000043	0.9848
	MNN	-1.59E-06	0.0103	0.7668
	CP	-0.025	0.1056	0.3295
Bushland	MPS	1.61E-05	0.4254	0.0296*
	PD	-0.0146	0.4413	0.0258*
	MNN	-8.26E-05	0.1228	0.2908
	CP	0.0228	0.4904	0.0164*
Woodland	MPS	-0.0014	0.5644	0.0077*
	PD	0.0048	0.0682	0.4379
	MNN	1.23E-05	0.008	0.7943
	CP	-0.0365	0.68	0.0031*

n=11, corresponding to the management block spatial units.

*****Regression is significant at the 0.05 level.

3.3.4 Landscape heterogeneity change in relation to spatial rainfall variability

Table 3.3 illustrates that overall there are no significant relationships between measures of landscape heterogeneity change and spatial rainfall variability. The relationship is only statistically significant for grassland mean nearest neighbour distance (R^2 = 0.854, p = 0.019).

Table 3.3: Spatial Autoregressive (SAR) model results for the relationship between spatial rainfall variability and Mean Patch Size (MPS), Patch Density (PD), Mean Nearest Neighbour Distance (MNN) and Class Proportion (CP)

Land Cover Type	Landscape Metrics	Coefficient	R^2	p-value
Grassland	MPS	-0.0728	0.8415	0.1746
	PD	-0.4900	0.8340	0.9124
	MNN	-0.0035	0.8535	0.0194*
	CP	-9.7278	0.8378	0.3775
Bushland	MPS	-0.0011	0.8344	0.6974
	PD	0.6466	0.8348	0.8108
	MNN	0.0055	0.8343	0.9051
	CP	1.5139	0.8342	0.8254
Woodland	MPS	0.0182	0.8374	0.4908
	PD	-0.4379	0.8344	0.9124
	MNN	0.0097	0.8363	0.2899
	CP	3.0952	0.8358	0.7056

n=40, corresponding to polygons representing eight rainfall spatial classes.

*****Regression is significant at the 0.05 level.

3.4 Discussion

Results of this study indicate that elephant density is positively influenced by availability of surface water in the late dry season. This implies the distribution of surface water in the late dry season significantly influences the spatial distribution of elephants across the landscape. As per expectation, as waterhole density increases, concentration of elephants also increases and this relationship is stronger for areas where late dry season waterholes still hold water. The result of this study is consistent with the findings of Chamaillé-Jammes et al. (2007c) in HNP that infer strong association between density of artificial waterholes and elephant densities. Nevertheless, it can be deduced that this is the first time this hypothesis has been tested in a spatially explicit way, providing a more efficient way of assessing density of elephants in relation to availability of surface water resources across landscape units.

While availability of surface water significantly influences the distribution of elephants in the landscape there are other factors that drive elephant movement patterns and distribution across the landscape. Elephants are selective when foraging, foraging and movement patterns which also determine their distribution is influenced by vegetation type with elephants showing preference for habitats with high proportions of vegetation (Harris et al., 2008) and which are more heterogeneous (Grainger et al., 2005; De Beer and Van Aarde, 2008). Elephant distribution is also influenced by substrate fertility where nutrient rich plants on nutrient rich soils are preferred (Harris et al., 2008; Asner and Levick, 2012). Seasonality, plant phenology and plant greenness (Loarie et al., 2009) are also key drivers of elephant foraging and movement patterns and elephants also show preference for certain woody plant species (O'Connor et al., 2007). The influence of these intricate factors also account for the distribution and density of elephants in the landscape. However, the distribution of surface

water in the late dry season can also influence elephant foraging decisions especially when water becomes a limiting factor and elephants are constrained to forage close to water sources or in areas with a dense network of waterholes so that they are able to adequately meet both their drinking and foraging needs.

Results on the short term effect of elephant density on vegetation heterogeneity indicate that there are no significant changes in vegetation heterogeneity in the dry season due to elephant densities which could be detected using Landsat-derived NDVI CoV. This is contrary to the expectation that areas with high elephant densities in the late dry season would show a high magnitude of change in NDVI CoV in the late dry season. Studies done by Fullman and Bunting, (2014) in Chobe National Park Botswana, showed that in regions where there was intensive elephant utilisation impact the moving standard deviation index of vegetation spectral indices was high. As elephants forage, inevitably there is breaking of branches and significant removal of plant biomass and in some instances toppling of trees (Hiscocks, 1999). Differences in sensitivity and response of different vegetation types to elephant browsing could also explain the lack of significant changes. For example areas dominated by high woody cover might show a low magnitude of change in response to elephant browsing effects in the short term as effects can be masked, whereas areas predominated by low woody cover might be more sensitive to browsing effects and show a greater magnitude of change due to the more open background. Occupancy in a habitat by elephants is driven by variable factors determining forage quality and intensity vary in different localities across the landscape and therefore vegetation heterogeneity change may fail to respond linearly to elephant densities at the landscape scale (Timberlake and Childes 2004; Shrader, 2012). Therefore this study provides notable insight that in the short term no significant changes to

vegetation heterogeneity can be detected in savanna woodlands as a result of varying elephant densities at the landscape scale; however there is need to test consistency of this result in other ecosystems.

When analysed using satellite remotely-sensed method, the result of this study provide evidence of considerable elephant density mediated effects on landscape heterogeneity change driven by artificial waterholes in the long term. Results indicate that mean patch size for woodland decreases while mean patch size for bushland increases and patch density for bushland decreases as density of artificial waterholes increases. This result strongly suggests that there is structural conversion of trees to shrubs at edges of woodland patches which leads to shrinking of woodland patches and merging of the original and transformed bushland patches, thereby altering heterogeneity of the landscape. Results of this study indicate that woodland class proportion decreases while bushland class proportion increases with increasing density of artificial waterholes across the landscape. It can be inferred that due to heavy browsing by elephants, there are long-term structural changes to woodland where trees (Barnes, 1982) are converted to shrubs through coppicing (Mapaure and Mhlanga, 2000; Rutina et al., 2005; Kerley et al., 2008) thereby severely altering landscape structure by homogenising woody vegetation in the landscape in areas with high artificial waterhole density.

Results of this study provide evidence that consistently high elephant disturbance in the long-term alters landscape composition towards bushland (Styles and Skinner, 1997). This finding is consistent with deductions made by Teren (2016) in Linyati woodland, northern Botswana, where in the long term (16-18 years) elephant impact resulted in tall canopy tree woodland

being replaced by shrubland. Studies done at the micro scale in Kruger National Park (Trollope et al., 1998) also suggested that changes in woody vegetation involved a change in structural diversity where woody vegetation is transformed to bushland. In this study from land cover maps it can also be asserted that there are other factors other than water-driven elephant densities influencing major changes in landscape heterogeneity in the long term, mainly in the conversion of bushland to grassland, thereby inhibiting homogenisation of vegetation to bushland. Results of this study provide evidence that at high densities elephants induce structural change in woodland patches as they are converted to bushland; however this could be facilitating forage availability at lower height strata for other smaller browsers (Kerley et al., 2008). In turn, other smaller browsers could be responsible for the conversion of bushland to grassland (Rutina et al., 2005) at the landscape scale in HNP.

In this study the influence of spatial rainfall variability on landscape heterogeneity change was also evaluated, where a natural east west gradient of decreasing rainfall also affects vegetation productivity (Chamaillé-Jammes et al., 2009a). Results of this study show that spatial rainfall variability has negligible influence on magnitude of landscape heterogeneity change. The only significant relationship was of decreasing distance between grassland patches with increasing rainfall which may infer the influence of spatial rainfall variability on grassland spatial arrangement. It can therefore be deduced that spatial rainfall variability has minimum influence on the noticeable landscape heterogeneity change in the long-term.

This study is unique in that assessments and ecological conclusions on both the short term effects of elephant density and long term effects of elephant densities through artificial waterholes on landscape heterogeneity could be made using multi-temporal spectral data

covering a large spatial extent rather than relying only on ground data which is limited in temporal and spatial extent. Previous studies have mostly assessed vegetation change around artificial waterholes 'piosphere effect' at fine spatial scales (Thrash, 1998; Brits 2002; Makhabu et al., 2002; Landman et al., 2012; Mukwashi et al., 2012), however this study provides evidence that elephant density effects are not only considerable at vicinities close to waterholes but are larger in extent with significant elephant-induced change as a result of artificial waterholes being observed at the landscape scale. It can be concluded that maintenance of high elephant densities in the long term indicates that woodland will be transformed to bushland which could be detrimental to wildlife species' habitat (Murwira and Skidmore, 2005; Tews et al., 2004) and maintaining biodiversity (Guldemond et al., 2017). However, the coppiced bushland provides a favourable habitat for other herbivores which are speculated to be transforming bushland to grassland thereby enhancing overall vegetation heterogeneity in the protected area. It can, however, be recommended that in protected areas surface water provision can be a useful tool for regulating landscape structure mostly on the long term where the changes are most significant i.e. closing some waterholes in a series of years to allow shrub recruitment into woodland, thereby regulating structural diversity of woody vegetation.

Chapter 4: Understanding effects of water-driven elephant densities on landscape heterogeneity change using GIS and remote sensing techniques: A Synthesis

---

4.1 Introduction

The relationship between elephant density and landscape heterogeneity change is complex and is largely dependent on a number of interacting factors which drive elephant distribution across space and time (Van Aarde et al., 2006; Balfour et al., 2007). These complex factors include the longevity of elephants, the large scales at which they use landscapes, the temporal and spatial scales of responses of ecosystems affected by elephants (Kerley et al., 2008), as well as the spatial distribution of landscape resources (Balfour et al 2007; Kerley et al., 2008). It is also mainly acknowledged that part of the problem in assessing landscape heterogeneity change and determining their related factors originate from the difficulty in monitoring vegetation on a big enough scale and long enough time to detect and distinguish trends from cycles and complex dynamic processes (Western, 2007). Thus, adopting methods to monitor vegetation changes at large spatial scales as well as large temporal extents is invaluable.

Remote sensing provides an invaluable source of spatial data which covers large spatial extents and long temporal scales to better understand the contribution of elephant density on landscape heterogeneity change and therefore make comprehensive ecological deductions. Maintaining heterogeneity is critical to the functioning of savanna ecosystems (Beale et al.,

2013) therefore effective monitoring of surface water resources, elephant movement and distribution patterns and elephant-induced landscape heterogeneity change is crucial in the management of savanna ecosystems (Grant et al., 2011). To the best of our knowledge, there has been limited application of objective spatial methods for mapping and monitoring distribution of waterholes and quantifying landscape heterogeneity change as a result of elephant densities for management of semi-arid savanna ecosystems.

In this thesis, the main aim was to test the utility of GIS and remote sensing-based approaches to understand the effects of elephant density on landscape heterogeneity change around artificial waterholes in semi-arid savanna landscapes of southern Africa. The thesis specifically (1) developed an innovative method for objectively detecting waterholes and (2) related spatial distribution of these remotely-sensed waterholes to elephant density and assessed the density-related elephant effects as a result of artificial waterholes on landscape heterogeneity change using GIS and remote sensing methods.

4.2 Detecting and mapping waterholes based on an optimal threshold for MNDWI

The detection of waterholes forms a key basis to understanding elephant distribution patterns and density related elephant-induced landscape heterogeneity change (Stokke and du Toit, 2002; De Beer and van Aarde 2008; Junker et al., 2008). In this thesis, it was found that MNDWI is the better performing spectral water index which efficiently detects waterholes at an optimal threshold of -0.29 (Kappa coefficient was 0.85). This is one of the first few studies which tested for an objective method to detect and map waterholes and proposed an optimal threshold based on a robust remote sensing water index for detecting and mapping waterholes in semi-arid regions. Systematic detection of waterholes using a robust remote sensing

derived water index allows monitoring surface water availability at large-spatial and long-temporal extents in place of field-based waterhole monitoring which are constrained by time and cost and are therefore carried out at limited spatial and temporal scales.

4.3 Remote sensing application in assessing waterhole-elephant density dynamics and detecting elephant density effects on landscape heterogeneity change

Elephant densities are known to have differential effects on landscape heterogeneity change as a result of artificial waterholes in protected areas (Balfour et al., 2007; Guldemond and van Aarde, 2007; Grant et al., 2011). To test this hypothesis, this thesis used waterholes detected using MNDWI to relate elephant densities to late dry season surface water availability at the landscape scale. This is one of the first studies which tested waterhole-elephant density dynamics in a spatially explicit way, providing an efficient means of monitoring waterhole-herbivore density dynamics at the landscape scale which can guide in managing wildlife distribution patterns in protected areas.

Using NDVI CoV, landscape metrics and elephant density data from aerial survey counts in this study, it was found that in the short-term there are no significant changes to landscape heterogeneity as a result of different elephant density across the landscape. However, in the long-term at high densities, elephants transform woodland to bushland, which is consistent with predictions and observations made in previous studies (Cumming et al., 1997; Skarpe et al., 2004; Teren, 2016). Findings of this thesis imply that artificial waterholes can be useful in regulating heterogeneity of the landscape, it is suggested that artificial waterholes in areas with high artificial waterhole densities be closed in a series of years to moderate elephant

densities and allow bushland to recruit back to woodland. This thesis is distinctive in that comprehensive ecological deductions on the effect of elephant density as a result of artificial waterholes could be made using a GIS and remote sensing based approach at the landscape scale and at different time scales for guiding policy management of artificial waterholes. Understanding water-driven elephant density landscape heterogeneity change also provides a necessary basis for more advanced studies to better understand implications of landscape pattern change on other animal populations, their spatial distribution and their landscape pattern preference by using satellite images and animal GPS collar data.

4.4 Summary of findings

In this thesis a novel finding was that the optimal threshold for MNDWI that can be used for detecting waterholes in semi-arid regions of southern Africa is -0.29. This demonstrates that when objective criteria is used, remotely-sensed waterholes can be used to monitor surface water availability trends and waterhole-herbivore dynamics, which can guide decisions for management of wildlife distribution patterns. This thesis also demonstrated that remotely sensed NDVI CoV can successfully be used to measure elephant density mediated effects on landscape heterogeneity change in the short-term and landscape metrics (mean patch size, patch density, class proportion and nearest neighbour distance) can measure long-term elephant density effects on landscape heterogeneity change. In this thesis, it is concluded that GIS methods and remotely-sensed data can successfully be used to detect and map waterholes, assess waterhole dynamics and measure elephant density effects on landscape heterogeneity for sustainable management of semi-arid savanna ecosystems.

4.5 Recommendations for future research

While an optimum threshold was successfully used to detect waterholes, further research is needed in assessing whether this threshold is applicable to remotely-sensed data at different spatial resolutions. This study did not capture intra-seasonal hydrological dynamics of the waterholes, their drying and wetting episodes (Nhiwatiwa and Dalu, 2017), in response to rainfall variability. However, work done in this study provides the prerequisite foundation for future studies to assess hydrological dynamics associated with waterholes at the landscape scale. There is also need to come up with predictive models which can link rainfall to number of waterholes which take into account the finer detail of rainfall patterns (length of dry period in between rainfall episodes, length of the rainfall season and the number of waterholes present at different time lags in the wet and dry season) in coming up with well calibrated predictive models. It is also recommended that future studies done on small spatial scales further incorporate finer detail of geomorphological characteristics of waterholes and assess how this influences their response to spatio-temporal dynamics in rainfall. In this thesis, while evidence was provided that elephants are responsible for the transformation of woodland patches to bushland, there is need to determine the implication of elephant-induced landscape heterogeneity change on changes in wildlife diversity to fully understand the ecological impacts of elephant density and artificial waterholes on semi-arid savanna ecosystems. There is also need to investigate the temporal interval needed and regeneration capacity for bushland to recruit to tree woodland in considering reversing elephant-induced structural change to woody vegetation through the manipulation of artificial waterholes. In changing the distribution of artificial waterholes through closure or new placement which will consequently change the distribution and impact of elephants, there is also need to understand the resilience capacity of the different landscape areas which can accommodate high elephant densities.

References

Anselin, L., (2006). GeoDa (software).

Anselin, L., Syabri, I. and Kho, Y. (2006). GeoDa: an introduction to spatial data analysis. *Geographical Analysis* **38**: 5–22.

Asadullah, A., McIntyre, N. and Kigobe, M. (2008). Evaluation of five satellite products for estimation of rainfall over Uganda/Evaluation de cinq produits satellitaires pour l'estimation des precipitations en Ouganda. *Hydrological Sciences Journal* **53**: 1137–1150.

Asner, G.P. and Levick, S.R. (2012). Landscape scale effects of herbivores on treefall in African savannas. *Ecology letters* **15**: 1211–1217.

Ayana, E.K., Philpot, W.D., Melesse, A.M. and Steenhuis, T.S. (2015). Assessing the potential of MODIS/Terra version 5 images to improve near shore lake bathymetric surveys. *International Journal of Applied Earth Observation and Geoinformation* **36**: 13–21.

Baldi, G. and Paruelo, J.M. (2008). Land-use and land cover dynamics in South American temperate grasslands. *Ecology and Society* **13**: 1–21.

Balfour, D., Dublin, H.T., Fennessy, J., Gibson, D., Niskanen, L. and Whyte, I.J. (2007). *Review of Options for Managing the Impacts of Locally Overabundant African Elephants*. IUCN, Gland, Switzerland.

Barnes, R.F.W. (1982). Elephant feeding behaviour in Ruaha National Park, Tanzania. *African Journal of Ecology* **20**: 123–136.

Beale, C.M., van Rensberg, S., Bond, W.J., Coughenour, M., Fynn, R., Gaylard, A., Grant, R., Harris, B., Jones, T. and Mduma, S. (2013). Ten lessons for the conservation of African savannah ecosystems. *Biological conservation* **167**: 224–232.

Bochow, M., Heim, B., Küster, T., Rogaß, C., Bartsch, I., Segl, K., Reigber, S. and Kaufmann, H. (2012). On the use of airborne imaging spectroscopy data for the automatic detection and delineation of surface water bodies. In: Chemin Y, editor. *Remote Sensing of Planet Earth*. Rijeka, Croatia: InTech pp. 3–22.

Brits, J., Van Rooyen, M.W. and Van Rooyen, N. (2002). Ecological impact of large herbivores on the woody vegetation at selected watering points on the eastern basaltic soils in the Kruger National Park. *African Journal of Ecology* **40**: 53–60.

Bruce, C.M. and Hilbert, D.W. (2006). *Pre-processing methodology for application to Landsat TM/ETM+ imagery of the wet tropics*. Rainforest CRC.

Cantor ,S.B., Sun, C.C., Tortolero-Luna, G., Richards-Kortum, R. and Follen, M. (1999). A comparison of C/B ratios from studies using receiver operating characteristic curve analysis. *Journal of Clinical Epidemiology* **52**: 885–892.

Chamaillé-Jammes, S., Charbonnel, A., Dray, S. and Madzikanda, H., Fritz, H. (2016). Spatial distribution of a large herbivore community at waterholes: an assessment of its stability over years in Hwange National Park, Zimbabwe. *PloS One* **11**: e0153639.

Chamaillé-Jammes, S., Fritz, H. and Madzikanda, H. (2009a). Piosphere contribution to landscape heterogeneity: a case study of remote-sensed woody cover in a high elephant density landscape. *Ecography* **32**: 871–880.

Chamaillé-Jammes, S., Valeix, M., Bourgarel, M., Murindagomo, F. and Fritz, H. (2009b). Seasonal density estimates of common large herbivores in Hwange National Park, Zimbabwe. *African Journal of Ecology* **47**: 804–808.

Chamaillé-Jammes, S., Fritz, H. and Murindagomo, F. (2007a). Climate-driven fluctuations in surface-water availability and the buffering role of artificial pumping in an African savanna : Potential implication for herbivore dynamics. *Austral Ecology* **32**: 740–748. doi: 10.1111/j.1442-9993.2007.01761.x.

Chamaillé-Jammes ,S., Fritz, H. and Murindagomo, F. (2007b). Detecting climate changes of concern in highly variable environments: Quantile regressions reveal that droughts worsen in Hwange National Park, Zimbabwe. *Journal of Arid Environments* **71**: 321–326. doi: 10.1016/j.jaridenv.2007.05.005.

Chamaillé-Jammes, S., Valeix, M. and Fritz, H. (2007c). Managing heterogeneity in elephant distribution : interactions between elephant population density and surface-water availability. *Journal of Applied Ecology* **44**: 625–633. doi.org/10.1111/j.1365-2664.2007.01300.x

Chander, G. and Markham, B. (2003). Revised Landsat-5 TM radiometric calibration procedures and postcalibration dynamic ranges. *IEEE Transactions on geoscience and remote sensing* **41**: 2674–2677.

Coppin, P., Jonckheere, I., Muys, B. and Lambin, E. (2004). Digital change detection methods in ecostem monitoring: a review. *International Journal of Remote Sensing* **25**: 1565–1596. doi: 10.1080/0143116031000101675.

Cronje, H.P., Cronje, I. and Botha, A.J. (2005). The distribution and seasonal availability of surface water on the Manyeleti Game Reserve, Limpopo Province, South Africa. *Koedoe* **48**: 11–21.

Cumming, D.H., Fenton, M.B., Rautenbach, I.L., Taylor, R.D., Cumming, G.S., Cumming, M.S., Dunlop, J.M., Ford, A.G., Hovorka, M.D. and Johnston, D.S. (1997). Elephants, woodlands and biodiversity in southern Africa. *South African Journal of Science* **93**: 231–236.

Davidson, Z., Valeix, M., Van Kesteren, F., Loveridge, A.J., Hunt, J.E., Murindagomo, F. and Macdonald, D.W. (2013). Seasonal diet and prey preference of the African lion in a waterhole-driven semi-arid savanna. *PLoS One* **8**: e55182.

Davies, C. (1996). Aerial census of elephant and other large mammals in the Gonarezhou, Zambezi Valley, north-west Matabeleland, Sebungwe, Dande and Communal Land regions of Zimbabwe, July to November 1995. *Department of National Parks and Wildlife Management, Zimbabwe.*

De Beer, Y., Van Aarde, R. (2008). Do landscape heterogeneity and water distribution explain aspects of elephant home range in southern Africa's arid savannas? *Journal of Arid Environments* **72**: 2017–2025.

Deus, D. and Gloaguen, R. (2013). Remote sensing analysis of lake dynamics in semi-arid regions: Implications for water resource management. Lake Manyara East African Rift, Northern Tanzania. *Water* **5**: 698–727. doi: 10.3390/w5020698.

Du, Z., Linghu, B., Ling, F., Li, W., Tian, W., Wang, H., Gui, Y., Sun, B. and Zhang, X. (2012). Estimating surface water area changes using time-series Landsat data in the Qingjiang River Basin, China. *Journal of Applied Remote Sensing* **6**: 1–16.

Dublin, H.T. (1995). Vegetation dynamics in the Serengeti-Mara ecosystem: the role of elephants, fire, and other factors. Serengeti II: dynamics, management, and conservation of an ecosystem. *University of Chicago Press, Chicago* 71–90.

Dudley, J.P., Criag, G.C., Gibson, D.S.C., Haynes, G. and Klimowicz, J. (2001). Drought mortality of bush elephants in Hwange National Park, Zimbabwe. *African Journal of Ecology* **39**: 187–194.

Dzinotizei, Z., Murwira, A., Zengeya, F.M. and Guerrini, L. (2017). Mapping waterholes and testing for aridity using a remote sensing water index in a southern African semi-arid wildlife area. *Geocarto International* 1–13.

Eiden, G., Kayadjanian, M. and Vidal, C. (2000). Capturing landscape structures: Tools. *From land cover to landscape diversity in the European Union* 7–15.

El-Asmar, H.M., Hereher, M.E. and El Kafrawy, S.B. (2013). Surface area change detection of the Burullus Lagoon, North of the Nile Delta, Egypt, using water indices: A remote sensing approach. *Egyptian Journal of Remote Sensing and Space Science* **16**: 119–123.

ESRI, (2014). ArcGIS 10.2. 1 for Desktop. Environmental System Research Institute. Redlands, CA.

ESRI, (2002). ArcView GIS 3.2. Environmental Systems Research Institute, Redlands, CA.

Feyisa, G.L., Meilby, H., Fensholt, R. and Proud, S.R. (2014). Automated water extraction index: a new technique for surface water mapping using Landsat imagery. *Remote Sensing of Environment* **140**: 23–35.

FGDC (Federal Geographic Data Committee), (1997). National Vegetation Classification Standard. US Geological Survey, 590 National Center, Reston, Virginia.

Fichera, C.R., Modica, G. and Pollino, M. (2012). Land Cover classification and change-detection analysis using multi-temporal remote sensed imagery and landscape metrics. *European Journal of Remote Sensing* **45**: 1–18.

Freitag-Ronaldson, S. and Foxcroft, L.C. (2003). Anthropogenic influences at the ecosystem level. *The Kruger Experience: ecology and management of savanna heterogeneity* 391–421.

Fullman, T.J. and Bunting, E.L. (2014). Analyzing vegetation change in an elephant-impacted landscape using the moving standard deviation index. *Land* **3**: 74–104.

Fullman, T.J. and Child, B. (2012). Water distribution at local and landscape scales affects tree utilization by elephants in Chobe National Park, Botswana. *African Journal of Ecology* 1–9.

Gautam, V.K., Gaurav, P.K., Murugan, P. and Annadurai, M. (2015). Assessment of surface water dynamics in Bangalore using WRI, NDWI, MNDWI, Supervised classification and K-T transformation. *Aquatic Procedia* **4**: 739–746.

Gaylard, A., Owen-Smith, N. and Redfern, J. (2003). Surface water availability: implications for heterogeneity and ecosystem processes. *The Kruger experience: ecology and management of savanna heterogeneity. Washington: Island Press* pp. 171–188.

Gebremichael, M. and Hossain, F. (2010). *Satellite rainfall applications for surface hydrology*. Netherlands: Springer.

Grainger, M., Van Aarde, R. and Whyte, I. (2005). Landscape heterogeneity and the use of space by elephants in the Kruger National Park, South Africa. *African Journal of Ecology* **43**: 369–375.

Grant, R.C., Peel, M.J., Bezuidenhout, H. (2011). Evaluating herbivore management outcomes and associated vegetation impacts. *Koedoe* **53**: 116–130.

Guldemond, R.A.R., Purdon, A. and Van Aarde, R.J. (2017). A systematic review of elephant impact across Africa. *PLoS One* **12**: e0178935.

Guldemond, R, van Aarde, R. (2007). The impact of elephants on plants and their community variables in South Africa's Maputaland. *African Journal of Ecology* **45**: 327–335.

Harris, G.M., Russell, G.J., van Aarde, R.I. and Pimm, S.L. (2008). Rules of habitat use by elephants Loxodonta africana in southern Africa: insights for regional management. *Oryx* **42**: 66–75.

Helsel, D.R. and Hirsch, R.M. (1993). *Statistical methods in water resources*. USA: Elsevier Science.

Hiscocks, K.A.Y. (1999). The impact of an increasing elephant population on the woody vegetation in southern Sabi Sand Wildtuin, South Africa. *Koedoe* **42**: 47–55.

Holdo, R.M., Holt, R.D. and Fryxell, J.M. (2009). Grazers, browsers, and fire influence the extent and spatial pattern of tree cover in the Serengeti. Ecological Applications **19**: 95–109.

Hui, F., Xu, B., Huang, H., Yu, Q. and Gong, P. (2008). Modelling spatial-temporal change of Poyang Lake using multitemporal Landsat imagery. *International Journal of Remote Sensing* **29**: 5767–5784. doi: 10.1080/01431160802060912.

ITT, 2013. ENVI 5.1. *ITT Industries Inc, Colorado.*

Jenness, J., Wynne, J. (2006). Kappa analysis extension for ArcView 3. x.(version 2.1). *Flagstaff: Jenness Enterprises*. *Retrieved January 26, 2009.*

Ji, L., Zhang, L. and Wylie, B. (2009). Analysis of dynamic thresholds for the Normalized Difference Water Index. *Photogrammetric Engineering and Remote Sensing* **75**: 1307–1317.

Junker, J., van Aarde, R.J., Ferreira, S.M. (2008). Temporal trends in elephant Loxodonta africana numbers and densities in northern Botswana: is the population really increasing? *Oryx* **42**: 58–65.

Kalwij, J.M., de Boer, W.F., Mucina, L., Prins, H.H.T., Skarpe, C. and Winterbach, C. (2010). Tree cover and biomass increase in a southern African savanna despite growing elephant population. *Ecological Applications* **20**: 222–233. doi.org/10.1890/09-0541.1.

Kaptué, A.T., Hanan, N.P. and Prihodko, L. (2013). Characterization of the spatial and temporal variability of surface water in the Soudan-Sahel region of Africa. *Journal of Geophysical Research: Biogeosciences* **118**: 1472–1483. doi: 10.1002/jgrg.20121.

Kerley, G.I., Landman, M., Kruger, L., Owen-Smith, N., Balfour, D., De Boer, W., Gaylard, A., Lindsay, K., Slotow, R. (2008). Effects of elephants on ecosystems and biodiversity, in: *Elephant Management; a Scientific Assessment for South Africa.* Wits University Press, pp. 146–205.

Knight, J.F. and Lunetta, R.S. (2003). An experimental assessment of minimum mapping unit size. *IEEE Transactions on Geoscience and Remote Sensing* **41**: 2132–2134.

Landman, M., Schoeman, D.S., Hall-Martin, A.J. and Kerley, G.I.H. (2012). Understanding long-term variations in an elephant piosphere effect to manage impacts. *PLoS One* **7**: 1–11. doi: 10.1371/journal.pone.0045334.

Li, W., Du, Z., Ling, F., Zhou, D., Wang, H., Gui, Y., Sun, B. and Zhang, X. (2013). A comparison of land surface water mapping using the normalized difference water index from TM, ETM+ and ALI. *Remote Sensing* **5**: 5530–5549.

Lindquist, E.J. and D'Annunzio, R. (2016). Assessing Global Forest Land-Use Change by Object-Based Image Analysis. *Remote Sensing* **8**: 678–695.

Liu, C., Berry, P.M., Dawson, T.P. and Pearson, R.G. (2005). Selecting thresholds of occurrence in the prediction of species distribution. *Ecography* **28**: 385–393.

Loarie, S.R., van Aarde, R.J. and Pimm, S.L. (2009). Elephant seasonal vegetation preferences across dry and wet savannas. *Biological Conservation* **142**: 3099–3107.

Makhabu, S.W., Marotsi, B. and Perkins, J. (2002). Vegetation gradients around artificial water points in the Central Kalahari Game Reserve of Botswana. *African Journal of Ecology* **40**: 103–109.

Mapaure, I. and Mhlanga, L. (2000). Patterns of elephant damage to Colophospermum mopane on selected islands in Lake Kariba, Zimbabwe. *Kirkia* 189–198.

Mapfumo, R.B., Murwira, A., Masocha, M. and Andriani, R. (2017). Detection of subtle deforestation due to logging using satellite remote sensing in wet and dry savanna woodlands of Southern Africa. *Geocarto International* **32**: 514–530.

Mariani, S. and Fauzi, F. (2017). The ArcView and GeoDa application in optimization of spatial regression estimate. *Journal of Theoretical & Applied Information Technology* **95**: 1102 - 1115.

McCoy, R.M. (2005). *Field methods in remote sensing*. London: Guilford Press.

McFeeters, S.K. (1996). The use of the Normalized Difference Water Index (NDWI) in the delineation of open water features. *International Journal of Remote Sensing* **17**: 1425–1432.

McGarigal, K. and Marks, B.J. (1995). Spatial pattern analysis program for quantifying landscape structure. Gen. Tech. Rep. PNW-GTR-351. *US Department of Agriculture, Forest Service, Pacific Northwest Research Station.*

Mosugelo, D.K., Moe, S.R., Ringrose, S. and Nellemann, C. (2002). Vegetation changes during a 36-year period in northern Chobe National Park, Botswana. *African Journal of Ecology* **40**: 232–240.

Mukwashi, K., Gandiwa, E. and Kativu, S. (2012). Impact of African elephants on Baikiaea plurijuga woodland around natural and artificial watering points in northern Hwange National Park, Zimbabwe. *International Journal of Environmental Sciences* **2**: 1355–1368.

Murwira, A. and Skidmore, A.K. (2005). The response of elephants to the spatial heterogeneity of vegetation in a Southern African agricultural landscape. *Landscape Ecology* **20**: 217–234.

Mutowo, G. and Murwira, A. (2012). Relationship between remotely sensed variables and tree species diversity in savanna woodlands of Southern Africa. *International Journal of Remote Sensing* **33**: 6378–6402.

Murthy, M.S.R., Giriraj A. and Dutt C.B.S. (2003). Geoinformatics for biodiversity assessment. *Biological letter* **40**: 75–100.

Nhiwatiwa, T., Dalu, T. (2017). Seasonal variation in pans in relation to limno-chemistry, size, hydroperiod, and river connectivity in a semi-arid subtropical region. *Physics and Chemistry of the Earth, Parts A/B/C* **97**: 37–45.

Nigro, J., Slayback, D., Policelli, F. and Brakenridge, G.R. (2014). NASA/DFO MODIS near real-time (NRT) global flood mapping product evaluation of flood and permanent water detection. *Evaluation, Greenbelt, MD.*

Norton-Griffiths, M. (1978). Counting animals. Serengeti Ecological Monitoring Programme, African Wildlife Leadership.

Nussbaum, E.M. (2014). *Categorical and nonparametric data analysis: choosing the best statistical technique*. New York: Routledge.

O'Connor, T.G., Goodman, P.S. and Clegg, B. (2007). A functional hypothesis of the threat of local extirpation of woody plant species by elephant in Africa. *Biological Conservation* **136**: 329–345.

Oindo, B.O. and Skidmore, A.K. (2002). Interannual variability of NDVI and species richness in Kenya. *International Journal of Remote Sensing* **23**: 285–298.

Oldeland, J., Wesuls, D., Rocchini, D., Schmidt, M. and Jürgens, N. (2010). Does using species abundance data improve estimates of species diversity from remotely sensed spectral heterogeneity? *Ecological Indicators* **10**: 390–396.

O'Neill, R.V., Riitters, K.H., Wickham, J. and Jones, K.B. (1999). Landscape pattern metrics and regional assessment. *Ecosystem Health* **5**: 225–233.

Owen-Smith N., Kerley G.I.H., Page B., Slotow R. and Van Aarde R.J. (2006). A scientific persepective on the management of elephants in Kruger National Park and elsewhere. *South African Journal of Science* **102**: 389–394.

Owen-Smith, N. (1996). Ecological guidelines for waterpoints in extensive protected areas. *South African Journal of Wildlife Research* **26**: 107–112.

Rempel, R.S. and Carr, A.P. (2003). Patch Analyst extension for ArcView: version 3. *Available on line at: http://flash. lakeheadu. ca/~ rrempel/patch/index. html.*

Rocchini, D., Balkenhol, N., Carter, G.A., Foody, G.M., Gillespie, T.W., He, K.S., Kark, S., Levin, N., Lucas, K. and Luoto, M. (2010). Remotely sensed spectral heterogeneity as a proxy of species diversity: recent advances and open challenges. *Ecological Informatics* **5**: 318–329.

Rogan, J. and Chen, D. (2004). Remote sensing technology for mapping and monitoring land-cover and land-use change. *Progress in Planning* **61**: 301–325.

Rogers, C. (1993). Woody vegetation survey of Hwange National Park: a report prepared for the Department of National Parks and Wild Life Management, Zimbabwe. Zimbabwe:

Department of National Parks and Wild Life Management x, 176p.-illus.. En Plant records. Geog 5.

Rowlingson, B.S. and Diggle, P.J. (1993). Splancs: Spatial Point Pattern Analysis Code in S-Plus. *Computers and Geosciences* **19**: 627–655.

Rutchey, K. and Godin, J. (2009). Determining an appropriate minimum mapping unit in vegetation mapping for ecosystem restoration: a case study from the Everglades, USA. *Landscape Ecology* **24**: 1351.

Rutina, L.P., Moe, S.R., Swenson, J.E., Rutina, L.P., Moe, S.R., Swenson, J.E. and Loxodonta, J.E.E. (2005). Elephant *Loxodonta africana* driven woodland conversion to shrubland improves dry-season browse availability for impalas Aepyceros melampus. *Wildlife Biology* **11**: 207–213.

Sankaran, M., Hanan, N.P., Scholes, R.J., Ratnam, J., Augustine, D.J., Cade, B.S., Gignoux, J., Higgins, S.I., Le Roux, X., Ludwig, F. (2005). Determinants of woody cov21`er in African savannas. *Nature* **438**: 846–849.

Schneier-Madanes, G. and Courel, M. (2010). *Water and sustainability in arid regions: bridging the gap between physical and social sciences*. London: Springer Sciences.

Seloana, M.Q., Kruger, J.W., Potgieter, M.J. and Jordaan, J.J. (2017). Elephant damage to Sclerocarya birrea on different landscapes. *International Journal of Biodiversity and Conservation* **9**: 97–106.

Senay, G.B., Velpuri, N.M., Alemu, H., Pervez, S.M., Asante, K.O., Kariuki, G., Taa, A., Angerer, J. (2013). Establishing an operational waterhole monitoring system using satellite data and hydrologic modelling: Application in the pastoral regions of East Africa. *Pastoralism: Research, Policy and Practice* **3**: 20.

Shanahan, M. Shubert, W. and Scherer, C. (2013). *Climate change in Africa: a guidebook for journalists*. Paris, France: UNESCO.

Shannon, G., Matthews, W.S., Page, B.R., Parker, G.E. and Smith, R.J. (2009). The affects of artificial water availability on large herbivore ranging patterns in savanna habitats: a new approach based on modelling elephant path distributions. *Diversity and Distributions* **15**: 776–783.

Sharma, R.C., Tateishi, R., Hara, K. and Nguyen, L.V. (2015). Developing Superfine Water Index SWI for Global Water Cover Mapping Using MODIS Data. *Remote Sensing* **7**: 13807–13841. doi: 10.3390/rs71013807.

Shrader, A.M., Bell, C., Bertolli, L. and Ward, D. (2012). Forest or the trees: At what scale do elephants make foraging decisions? *Acta Oecologica* **42**: 3–10.

Shrader, Adrian M., Pimm, S.L. and Aarde, R.J. (2010). Elephant survival, rainfall and the confounding effects of water provision and fences. *Biodiversity and Conservation* **19**: 2235–2245. doi.org/10.1007/s10531-010-9836-7.

Simpson, N.O., Stewart, K.M. and Bleich, V.C. (2011). What have we learned about water developments for wildlife? Not enough! *California Fish Game* **97**: 190–209.

Singh, K.V., Setia, R., Sahoo, S., Prasad, A. and Pateriya, B. (2015). Evaluation of NDWI and MNDWI for assessment of waterlogging by integrating digital elevation model and groundwater level. *Geocarto International* **30**: 650–661. doi.org/10.1080/10106049.2014.965757.

Skarpe, C., Aarrestad, P.A., Andreassen, H.P., Dhillion, S.S., Dimakatso, T., du Toit, J.T., Halley, D., J., Hytteborn, H., Makhabu, S., Mari, M. (2004). The return of the giants: ecological effects of an increasing elephant population. *AMBIO: A Journal of the Human Environment* **33**: 276–282.

Smit, I.P.J. (2013). Systems approach towards surface water distibution in Kruger National Park, South Africa. *Pachyderm* **53**: 91–98.

Stokke, S., Du Toit, J.T. (2002). Sexual segregation in habitat use by elephants in Chobe National Park, Botswana. *African Journal of Ecology* **40**: 360–371.

Styles, C. V. and Skinner, J.D. (1997). Seasonal variations in the quality of mopane leaves as a source of browse for mammalian herbivores. *African Journal of Ecology* **35**: 254–265.

Teren, G. (2016). Elephants and woody plant diversity: spatio-temporal dynamics of the Linyanti woodland, northern Botswana. *PhD Dissertation, University of Witwatersrand, Johannesburg, South Africa.*

Teren, G. and Owen-Smith, N. (2010). Elephants and riparian woodland changes in the Linyanti region, northern Botswana. *Pachyderm* **47**: 18–25.

Tews, J., Brose, U., Grimm, V., Tielbörger, K., Wichmann, M., Schwager, M. and Jeltsch, F. (2004). Animal species diversity driven by habitat heterogeneity/diversity: the importance of keystone structures. *Journal of Biogeography* **31**: 79–92.

Thorne, V., Coakeley, P., Grimes, D. and Dugdale, G. (2001). Comparison of TAMSAT and CPC rainfall estimates with raingauges, for southern Africa. *International Journal of Remote Sensing* **22**: 1951–1974.

Thrash I. and Derry J.F. (1999). The nature and modelling of piospheres: a review. *Koedoe* **42**: 73–94.

Thrash, I. (1998). Impact of large herbivores at artificial watering points compared to that at natural watering points in Kruger National Park, South Africa. *Journal of Arid Environments* **38**: 315–324.

Timberlake, J.R. and Childes, S.L. (2004). Biodiversity of the Four Corners Area: Technical Reviews Volume Two (Chapter 5-15) Appendix 5-1: Plant Checklist. *Occasional Publications in Biodiversity* **15**: 196.

Trollope, W.S.W., Trollope, L.A., Biggs, H.C., Pienaar, D. and Potgieter, A.L.F. (1998). Long-term changes in the woody vegetation of the Kruger National Park, with special reference to the effects of elephants and fire. *Koedoe* **41**: 103–112.

Van Aarde, R.J. and Jackson, T.P. (2007). Megaparks for metapopulations: addressing the causes of locally high elephant numbers in southern Africa. *Biological Conservation* **134**: 289–297.

Van Aarde, R., Jackson, T., Ferreira, S. (2006). Conservation science and elephant management in southern Africa: Elephant conservation. *South African Journal of Science* **102**: 385–388.

Verpoorter, C., Kutser, T. and Tranvik, L. (2012). Automated mapping of water bodies using Landsat multispectral data. *Limnology and Oceanography: Methods* **10**: 1037–1050.

Walker, D., Epstein, H., Raynolds, M., Kuss, P., Kopecky, M., Frost, G., Daniëls, F., Leibman, M., Moskalenko, N., Matyshak, G. (2012). Environment, vegetation and greenness (NDVI) along the North America and Eurasia Arctic transects. *Environmental Research Letters* **7**: 015504.

Weiss, J.L., Gutzler, D.S., Coonrod, J.E.A. and Dahm, C.N. (2004). Long-term vegetation monitoring with NDVI in a diverse semi-arid setting, central New Mexico, USA. *Journal of Arid Environments* **58**: 249–272.

Weiss, E., Milich, L. (1997). Errors in a standard method for generating interannual NDVI coefficient of variation (CoV) images. *International Journal of Remote Sensing* **18**: 3743–3748.

Western, D. (2007). A half a century of habitat change in Amboseli National Park, Kenya. *African Journal of Ecology* **45**: 302–310.

Western, D. and Maitumo, D. (2004). Woodland loss and restoration in a savanna park: a 20 year experiment. *African Journal of Ecology* **42**: 111–121.

Whyte, I.J., Van Aarde, R.J. and Pimm, S.L. (2003). Kruger's elephant population: its size and consequences for ecosystem heterogeneity, in: *The Kruger Experience: Ecology and Management of Savanna Heterogeneity. Island, Washington, DC* pp. 332–348.

Xu, H. (2006). Modification of normalised difference water index (NDWI) to enhance open water features in remotely sensed imagery. *International Journal of Remote Sensing* **27**: 3025–3033. doi.org/10.1080/01431160600589179.

Young, K.D., Ferreira, S.M. and van Aarde, R.J. (2009). Elephant spatial use in wet and dry savannas of southern Africa. *Journal of Zoology* **278**: 189–205. doi: 10.1111/j.1469-7998.2009.00568.x.